Authors' Response to referee comments for 'An efficient approach for treating composition-dependent diffusion within organic particles'

Comments from referees are presented in blue, these are followed by author's response in green and changes to the manuscript are in red.

We thank both referees for their detailed and helpful comments. The resulting changes discussed below have improved the presentation, clarity and message of the paper.

Referee #1:

1. The authors mentioned water as an important plasticizer for organic particles. I think this is also one of the motivations to develop such a composition-dependent diffusion model. However, it appears that the proposed correction scheme cannot be directly applied to the water/organic aerosol system as the molar volume ratio is far from the 1:1 ratio assumed in the simulations. This caveat should be discussed more explicitly in the manuscript.

This is an important caveat given the relatively high abundance and high self-diffusion coefficient of water in the atmosphere. Consequently we have modified the text to express it with greater emphasis. In the discussion (page 16, line 19) we write:

The presented parameter values are therefore unable to reliably estimate diffusion when the molar volume ratio of components does not equal 1:1 (a value we chose arbitrarily). Parameter values account for changes to the diffusivity and diffusing distance due to partitioning of a semi-volatile component. The diffusing distance is dependent on component molar volume ratios, therefore when these are varied new parameters are required. For such systems, however, the presented parameterisation for the correction is valid. With different parameter values the parameterisation would be applicable to, for example, the case of diffusion in a mixture of water and organic material.

We note that our response to point 9 of referee #2 is relevant to this point.

2. It is not clear how the in-particle diffusion of the non-volatile component was considered in the model. It seems that Eq. 1 can be applied to both the semi-volatile and non-volatile components. If that is the case, does the value of D in Eq. 2 represent both D_sv and D_nv? This assumption is reasonable for the semi-volatile/non-volatile system discussed in this paper. These diffusivities, however, need to be treated separately if molecular sizes are vastly different (such as water/organics). Some more discussions would be helpful.

The authors appreciate that some measurements show diffusion coefficients to be correlated with molecular size. However, in a two-component system where diffusion occurs along a mole fraction gradient, i.e., there is net movement of both components, the diffusion process is coupled. In order to attain volume continuity when using a fixed coordinate reference frame, the diffusion coefficients of the two components are then equal. This is explained in the paper with the addition of the following lines to the method (page 4, line 5):

The model described below uses a stationary coordinate reference frame, which for an ideal binary system requires that each component have the same diffusivity, quantified by the diffusion coefficient. This is true regardless of the component molecular size, and is physically necessary to attain volume continuity (Taylor and Krishna, 1993; Krishna and Wesselingh, 1997). The mathematical proof for the necessity of symmetric diffusion coefficients in an ideal binary system (e.g. comprising components 1 and 2) begins with:

$$\frac{-\nabla C_1}{\nabla C_2} = \frac{V_{m,2}}{V_{m,1}}$$

where V_m is the molar volume and ∇C is the concentration gradient at the boundary where flux is being considered. Next, Fick's first law (which is equivalent to Fick's second law when flux is at steady state) can be expressed in terms of volumetric flux ($m^3\ s^{-1}$):

$$J_i = D_i \nabla C_i V_{m,i} A$$

where A is the area diffusion occurs over. The magnitude of volumetric flux has to be equivalent for both components in order to attain volume continuity. For a particle of finite volume this means mass continuity is also satisfied. With this stipulation and eq. 3, it can be seen that symmetric diffusion coefficients are physically necessary.

3. Page 2 Line 13: "Unlike gas-phase diffusion, which is already accounted for in regional-scale models by equations of gas/particle partitioning...". Equations of gas/particle partitioning not always account for gas-phase diffusion. Many models treat the gas/particle partitioning as equilibrium partitioning, i.e., gas-phase diffusion was not explicitly considered. However, it might be true that the timescale of gas phase diffusion is short enough compared to the typical time step in atmospheric models. Some models may use a dynamic gas/particle partitioning scheme where gas-particle mass transfer rates are taken into account. Please revise this sentence to be more specific.

This sentence was considered to be unnecessary, and was removed with a slight modification of the following sentences to draw an appropriate link to regional-scale models (page 2, line 13):

To date particle-phase diffusion has not been included in regional-scale atmospheric models. Two outcomes of recent studies, however, indicate that particle-phase diffusion may pose a limitation to mass transfer over the timescales relevant to these models.

4. Page 6 Line 3: The meaning of "ve Δxs,sv" is not clear. What does "ve" stand for? Some descriptions for "+ve Δxs,sv" and "-ve Δxs,sv" might be needed in the caption of figure 1, too (condensation and evaporation?).

The authors agree. The method has been changed to (page 6, line 4):

i) constant $x_{s,sv,eq}$, with initial/equilibrium $x_{s,sv} = 0$ for positive (+ve, i.e. condensing case) $\Delta x_{s,sv}$ / negative (−ve, i.e. evaporating case) $\Delta x_{s,sv}$

and figure 1 caption has been changed to (page 6):

Figure 1. The shell resolution (given in the legend) distribution with $\Delta x_{s,sv}$ and $\log 10(D_{nv}^{0}/D_{sv}^{0})$ used, for: a) positive (+ve) $\Delta x_{s,sv}$ and b) negative (-ve) $\Delta x_{s,sv}$.

5. Figure 3: It appears that the value of correction factor can be large even there is no composition dependence of D (pink and green lines in Fig. 3). This inaccuracy due to changing particle size could be further emphasized in the discussions and conclusions, too.

We agree, and have added the following lines to the results and discussion, respectively (page 8, line 15):

Where the self diffusion coefficients of components are the same in fig. 3, the correction is required only for the changing particle size.

& (page 15 line 10)

The correction was required to account not only for variable diffusivity but also varying particle size as the semi-volatile component partitions between phases, since the uncorrected analytical solution assumes constant particle size.

Inaccuracy due to particle size is also mentioned in the edit regarding point 1 of referee #1.

6. Figure 9a: instead of showing the discrepancy between the models with/without the correction, I think it would be better to show the difference for each model with respect to the numerical solution. This may help the readers to understand how the results of composition-dependent model are improved compared with the model with a constant D.

The suggested changes were made to fig. 9a (page 13):

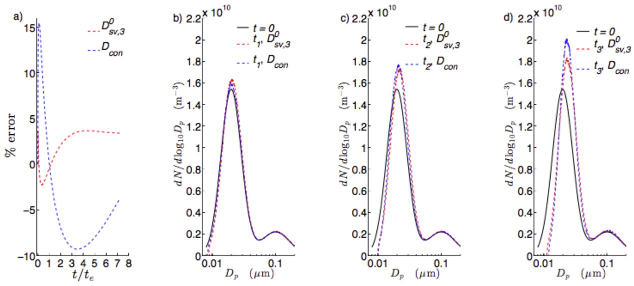

Figure 9. In a), the discrepancy (found using eq. 10) in estimated radius with model run time normalised to the *e*-folding time (t_e) when $x_{s,sv}$ is increased instantaneously from 0.00 to 0.88 for two diffusion coefficient treatments: i) corrected analytical solution with $D^0_{nv} = 1\text{x}10^{-26}$ and $D^0_{sv} = 1\text{x}10^{-22}$ m^2s^{-1} ($D^0_{sv,3}$) and ii) using the analytical without correction when D is constant at $4.4\text{x}10^{-23}$ m^2s^{-1} (D_{con}). In later plots are the number size distributions for the same diffusion coefficient treatments, with red representing the former treatment (variable D) and blue the latter one (constant D)). In b) $t = 2.4\text{x}10^4$ s, c) $t = 4.8\text{x}10^4$ s and in d) $t = 1.2\text{x}10^5$ s since simulation start.

Page 5 Line 14: "by a factor or e"->"by a factor of e"

Typographic error was corrected (page 5, line 24).

Referee #2

1. P. 1. L. 12-13: Authors state "Until such time as a general solution is found, caution should be given to sensitivity studies that assume constant diffusivity." I interpret this as a critique towards using constant diffusivity approach. However, as the authors themselves admit that they were not able to derive a general composition dependent description, it would seem to me that constant diffusivity assumption is better choice at the moment than using a composition dependence that might not be suitable for the given conditions.

This sentence in the abstract was presented without sufficient expansion in the main text. It is an important message because diffusivities measured at low relative humidities, for example, may not be applicable to the wider atmosphere where relative humidity and consequent water concentration in the particle-phase can change. We have added the following to the discussion so that a substitute to the constant diffusivity assumption is recommended (page 18, line 9):

In modelling studies where composition-dependent diffusion occurs and gas-phase saturation ratios of partitioning components vary over similar timescales to particle-phase diffusion, we recommend the numerical solutions mentioned above in preference to the assumption of constant diffusivity.

2. P. 5, L. 12-14: Authors chose e-folding state as the reference "time point". Did the authors test if the choice of this reference point affects the comparison results? Also, correct 'or' -> 'of' (L. 14)

Following this comment, models were run until the difference between surface and bulk concentration of the semi-volatile decreased by a factor of 16*e*. Although good agreement between the numerical and corrected analytical solutions was seen for the evaporating case this was not true for the condensation case. Consequently the correction equation used for the evaporation case was used and fitting was repeated, giving the new parameter values shown in table A3. These do give good agreement to this extended equilibrium point. Several changes resulted in the manuscript:

Figs. 3, 4, 5, 7, 8, 9 and 11 were reproduced with the new correction implemented.

New parameters in Table A1 and new interpolation method in Table A3.

Page 8, line 9:

The correction factor was then plotted against proximity to equilibrium; here we use the absolute difference between surface and bulk average x_{sv} . This process was done for the model inputs shown in fig. 1 to determine whether a general equation form could be found that described the relationship between the D correction factor (C_D) and proximity to equilibrium. Examples are shown in fig. 3. The resulting general equation for both +ve and -ve $\Delta x_{s,sv}$ is found to be:

$$C_D = e^{((|x_{s,sv} - x_{a,sv}|)^{p1})p2} - p_3,$$

where p_n is a parameter value, dependent on Δx and D^0_{nv} / D^0_{sv}.

The testing to an extended equilibrium point is now stated (page 8, line 29):

Corrected analytical and numerical solution results were also compared beyond the e-fold time, until the difference in concentration between surface and bulk had diminished to a factor of 16e. The agreement shown in fig. 4 was maintained to this further equilibration point.

3. P. 6, L. 7: It is stated that analytical solution was fit by eye to Fi-PaD results. Is fitting by eye enough accurate method for this? Why not using a more mathematical method for fitting the curve?

A more mathematical method was attempted through least squares fitting, however, it was found to be under constrained. We consider the assessment of fit through comparison of radius measurements to provide an objective means of assessing the accuracy of the correction. We have added the following text to the method to explain this (page 6, line 9):

To derive correction equations $R_p - t$ profiles estimated by the analytical solution were fit to those of Fi-PaD. A least squares fitting procedure was attempted and found to be under constrained, thus fitting was done by eye, and the quality of fit was objectively assessed through residuals, as described below.

4. P. 6, L. 11-12: It says "An interpolation method was developed to estimate parameters for the correction equation between the values of dxs,sv and log10(D0nv/D0sv) used for the equation derivation". This developed interpolation method needs to be described. I assume this refers to Tables A3 and A4. However, these tables and their captions require clarification. For instance, please clarify what it means when it says "whether the log10 of parameter values was taken" and "whether the log10 of the variable was taken" in the table captions.

The authors agree that greater explanation and clarity was needed for explaining the interpolation procedure. The following was added to the results (page 9, line 5):

The general method was to first interpolate with respect to $\Delta x_{s,sv}$ followed by D_{nv}^0 / D_{sv}^0. For most accurate results the interpolation equation was found to be dependent on the independent variables as described in the appendix (Tables A3 and A4). The interpolation was tested at $\Delta x_{s,sv}$ and D_{nv}^0 / D_{sv}^0 comparatively far from those with known parameter values and spread across the variable space.

and the table A3 caption was changed to (page 22):

Interpolation method for parameters in eq. 9 (for +ve $\Delta x_{s,sv}$). Interpolation is done with respect to $\Delta x_{s,sv}$ first, followed by $\log10(D_{nv}^0 / D_{sv}^0)$; the method for the former is given in the upper part of the table and the method for the latter is in the lower part. Note the method is dependent on the independent variable. Methods are represented by codes. The first number in each code is 1 if interpolation is done with respect to the $\log_{10}$ of parameter values, in which case the interpolation result must be raised to the power 10, and is 0 if no logarithm is taken. The second number in each code is 1 if the interpolation is done with respect to the $\log_{10}$ of the independent variable, and is 0 if no logarithm is taken. The final letter represents the form of the interpolation: L and S for linear and spline, respectively. For p_2, when interpolating with respect to $\log10(D_{nv}^0 / D_{sv}^0)$, the interpolation method depends on the value of this variable, which is denoted D^0.

and the table A4 caption was changed to (pag 22):

Interpolation method for parameters in eq. 9 (for -ve $\Delta x_{s,sv}$). Interpolation is done with respect to $\Delta x_{s,sv}$ first, followed by $\log 10(D^0_{nv}/D^0_{sv})$; the method for the former is given in the upper part of the table and the method for the latter is in the lower part. Note the method is dependent on the independent variable. Methods are represented by codes. The first number in each code is 1 if interpolation is done with respect to the $\log_{10}$ of parameter values, in which case the interpolation result must be raised to the power 10, and is 0 if no logarithm is taken. Because parameters are sometimes negative, to gain a real result from the logarithm, a constant must be added to the parameters first, if this is the case this constant is given in brackets beside the first code number (once interpolation is complete this constant is subtracted from the result after it has been raised to the power 10). The second number in each code is 1 if the interpolation is done with respect to the $\log_{10}$ of the independent variable, and is 0 if no logarithm is taken. The final letter represents the form of the interpolation: L and S for linear and spline, respectively. For p_2, when interpolating with respect to $\log 10(D^0_{nv}/D^0_{sv})$, the interpolation method depends on the value of this variable, which is denoted D^0_{rat}.

5. P. 7, L. 16-17: Why is the metric for proximity to equilibrium different for +ve and –ve cases?

Please see our response to referee #2, point 2

6. P. 12, L. 3-9 and Figure 9: Is the % error presented in Fig. 9a comparing analytical constant D version to Fi-PaD results or to analytical composition dependent D version? Based on text and use of eq. 9 it seems that comparison point would be Fi-PaD, but based on figure caption it sounds like comparison point is the analytical solution with composition dependent D.

Please see our response to referee #1, point 6.

7. P. 14, eq. 12: Please explain why was this particular functional form chosen for the p4.

There was insufficient explanation in the text of why a new equation was necessary for the case of varying surface mole fraction of the semi-volatile component. We have added the following to provide an explanation (page 14, line 11):

A new correction equation was required that could accommodate a variable surface mole fraction and give agreement with Fi-PaD estimates. Through fitting by eye this was found to be:

8. P. 15, L. 18-19: “In both solutions (numerical and analytical), diffusion rates have a square dependence on particle size”. If one substitutes eq. 6 to eq. 3 the diffusion rate in eq. 3 is dependent on Rp not Rp^2. Did the authors test the CD for different sizes?

This comment highlighted an omission in the original manuscript - the units for concentration in the particle-phase bulk for eq. 5 were not stated. They are mol m^-3 (air) rather than mol m^-3 (particle). This, and the result in terms of dependence of diffusion rate on particle size is stated in a modified paragraph following eq. 7 (previously eq. 5) (page 5, line 5):

where $_a$ represents the bulk of the particle-phase, $_g$ represents the gas-phase, j is the index for all components, m is the index for size-bin, R_p is particle radius, $C_g{}^*$ is the effective saturation vapour concentration (molm^{-3}(air)), C is the concentration in the bulk part of a phase (molm^{-3}(air)) and N is the particle number concentration (m^{-3}(air)). In order to compare results from eq. 1 and eq. 5, concentrations from the latter must be divided by the volume concentration of particles (m^3(particle)m^{-3}(air)). Following this division, it can be seen that diffusion has an inverse square dependence on particle radius in both solutions.

9. P. 15-16, from P. 15 L. 27 to P. 16 L. 3: If I understood correctly, the effect of different molar masses was tested by using the fitting parameter values that where determined from assuming both molar masses where 100 g/mol, and this CD did not work when M of semi-volatile was varying from that of non-volatile. Is it so that the correction factor CD simply doesn't work if M of compounds are different or would the CD work for the different M values if p parameters were fitted by using the M values that are of interest?

The CD would work for systems of different molar volume ratios than used here. We agree that this was not clearly stated. We have expressed this point better by modifying the discussion. We now say (page 16, line 19):

The presented parameter values are therefore unable to reliably estimate diffusion when the molar volume ratio of components does not equal 1:1 (a value we chose arbitrarily). Parameter values account for changes to the diffusivity and diffusing distance due to partitioning of a semi-volatile component. The diffusing distance is dependent on component molar volume ratios, therefore when these are varied new parameters are required. For such systems, however, the presented parameterisation for the correction is valid. With different parameter values the parameterisation would be applicable to, for example, the case of diffusion in a mixture of water and organic material.

We note that the same modification was used to address point 1 of referee #1.

Furthermore, line 18 of page 17 was changed to:

Along with the effect of component molar volume ratios on diffusion, however, this could be overcome through refitting of parameter values.

and line 20 of page 18 was changed to:

The verified correction is currently limited to conditions of similar molar volume between the partitioning component and the particle average, and of a logarithmic dependence of diffusion coefficient on partitioning component mole fraction. These limitations may be overcome through refitting of parameters.

10. P. 4, L. 24: Here it says subscript s refers to surface of particle, but eq. 3-5 do not contain subscript s. Is there a typo either in the equations or in the text?

This typo was fixed (now page 5, line 5).

11. P. 6, L. 3-4: Explain here what +ve and –ve mean.

This was done, as described in our response to point 4 of referee #1.

12. P. 13, L. 13 and Fig. 10: I recommend naming the x-curves with some other symbol than p. Use of p here is confusing as also the fitting parameters for CD are marked with p.

This was done, with p changed to prof (pages 14 and 15).

An efficient approach for treating composition-dependent diffusion within organic particles

Simon O'Meara[1], David O. Topping[1,2], Rahul A. Zaveri[3], and Gordon McFiggans[1]

[1]Centre for Atmospheric Science, School of Earth & Environmental Sciences, University of Manchester, Manchester, M13 9PL, UK

[2]National Centre for Atmospheric Science (NCAS), University of Manchester, Manchester, M13 9PL, UK

[3]Atmospheric Sciences and Global Change Division, Pacific Northwest National Laboratory, Richland, Washington 99352, USA

Correspondence to: Gordon McFiggans (g.mcfiggans@manchester.ac.uk)

Abstract.

Mounting evidence demonstrates that under certain conditions the rate of component partitioning between the gas- and particle-phase in atmospheric organic aerosol is limited by particle-phase diffusion. To date, however, particle-phase diffusion has not been incorporated to regional atmospheric models. An analytical rather than numerical solution to diffusion through organic particulate matter is desirable because of its comparatively small computational expense in regional models. Current analytical models assume diffusion to be independent of composition, and therefore use a constant diffusion coefficient. To realistically model diffusion, however, it should be composition-dependent (e.g. due to the partitioning of components that plasticise, vitrify or solidify). This study assesses the modelling capability of an analytical solution to diffusion corrected to account for composition dependence against a numerical solution. Results show reasonable agreement when the gas-phase saturation ratio of a partitioning component is constant and particle-phase diffusion limits partitioning rate ($< 10\%$ discrepancy in estimated radius change). However, when the saturation ratio of the partitioning component varies a generally applicable correction could not be found, indicating that existing methodologies are incapable of deriving a general solution. Until such time as a general solution is found, caution should be given to sensitivity studies that assume constant diffusivity. The correction was implemented in the polydisperse multi-process Model for Simulating Aerosol Interactions and Chemistry (MOSAIC), and is used to illustrate how the evolution of number size distribution may be accelerated by condensation of a plasticising component onto viscous organic particles.

1 Introduction

The accurate simulation of atmospheric aerosol transformation has been identified as a key component of assessing aerosol impact on climate and health (Jacobson and Streets, 2009; Fiore et al., 2012; Boucher et al., 2013; Glotfelty et al., 2016). However, comprehensive modelling of the physicochemical processes that determine aerosol transformation across large spatial and temporal scales can be challenging due to the limitations of computer power (Zaveri et al., 2008). While the majority of processes in large-scale models are solved by numerical methods, analytical solutions offer less computational expense. Particle-phase diffusion may be solved both analytically, under certain assumptions, or numerically (Crank, 1975).

The advantage of an analytical solution over a numerical one is the decreased computer expense (e.g. Smith et al., 2003; Zobrist et al., 2011; Shiraiwa et al., 2012). The Euler forward step method of Zobrist et al. (2011) was observed to have the shortest computer time of three published numerical methods for diffusion estimation (O'Meara et al., 2016). When a constant particle-phase diffusivity was assumed this method had a computer time approximately a factor of 20 greater than the analytical method presented in Zaveri et al. (2014) (with the numerical method using the minimum spatial resolution (20 shells) required for convergence of predicted equilibrium times, and the maximum change in component molecule number per time step recommended by Zobrist et al. (2011), while the analytical method used a conservative temporal resolution of $1\text{x}10^3$ time steps). To rigorously investigate the role of composition-dependent particle-phase diffusion in particulates containing organic components a multi-process large-scale model is required. An analytical-solution to particle-phase diffusion would make this much more practical than a numerical solution with respect to computer time.

~~Unlike gas-phase diffusion, which is already accounted for in regional-scale models by equations of gas/particle partitioning (Seinfeld and Pandis, 2006; Zaveri et al., 2008),~~ To date particle-phase diffusion has not ~~yet been included~~ been included in regional-scale atmospheric models. Two outcomes of recent studies, however, indicate that particle-phase diffusion may pose a limitation to mass transfer over the timescales relevant to these models. The first is field and laboratory observations that indicate organic particulates existing in a glassy phase state (Zobrist et al., 2008; Virtanen et al., 2010; Vaden et al., 2011; Saukko et al., 2012). Second is the contribution of very low volatility organic compounds (Ehn et al., 2014; Tröstl et al., 2016) to particulate matter, since volatility and diffusivity show positive correlations (Kroll and Seinfeld, 2008; Koop et al., 2011).

Whether particle-phase diffusion exerts a significant influence on the transformation of organic particulate matter remains an unanswered question. A major advance was the incorporation of an analytical solution to composition-independent particle-phase diffusion into a growth equation for a spherical particle by Zaveri et al. (2014). In examples of constant particle-phase diffusion coefficients, it was shown that, with sufficiently low diffusivity, particle number size distributions could be greatly perturbed, though there was also a dependency on reaction rate and volatility. Using both analytical and numerical solutions to mass transfer equations, Mai et al. (2015) also report particle-phase diffusion being limiting under certain conditions, with a dependency on accommodation coefficient, particle size, and volatility.

While the results of Zaveri et al. (2014) and Mai et al. (2015) are highly beneficial, they have not accounted for the possibility of composition-dependent diffusion (Vignes, 1966; Lienhard et al., 2014; Price et al., 2015; O'Meara et al., 2016). This is particularly relevant when considering the role of water, which is important because of its comparatively high abundance and high self-diffusion coefficient (Starr et al., 1999; O'Meara et al., 2016). The potential for water exerting a plasticising effect on low diffusivity organic particles is particularly important because the constituent components are expected to be highly oxidised (Ehn et al., 2014; Tröstl et al., 2016) and therefore polar and likely water soluble (Zuend et al., 2008; Topping et al., 2013). While numerical solutions to composition-dependent diffusion are available (Zobrist et al., 2011; Shiraiwa et al., 2012; O'Meara et al., 2016), an analytical solution has not, to the author's knowledge, yet been published. Indeed, Zaveri et al. (2014)

state that the analytical solution requires incorporation of further complexity in the particle-phase: heterogeneously distributed reactant species, liquid-liquid phase separation and heterogenous (with regard to position) diffusivity.

How does radial heterogeneity of diffusivity arise? Atmospheric component concentrations and their partitioning coefficients will vary substantially in time and space (Donahue et al., 2006), leading to concentration gradients through particles. With sufficient difference in the self-diffusivity of the component to the diffusivity of the particle bulk initially (in the case of condensation) or at equilibrium state (in the case of evaporation), and sufficient abundance of the component in the vapour-phase (condensation) or particle-phase (evaporation), diffusion is likely to occur at a rate dependent on particle composition. An example would be a particle predominately composed of secondary organic material with a low diffusivity that was formed during a comparatively low relative humidity afternoon and present in the boundary layer. Relative humidity increases as evening progresses and air temperature decreases. The resulting condensation of water onto the outside of the particle establishes a concentration gradient, thereby inducing diffusion. The increased concentration of water will act to increase diffusivity near the surface, whilst diffusivity in the particle core remains low (Zobrist et al., 2011; Lienhard et al., 2014; Price et al., 2015; O'Meara et al., 2016).

The analytical solution is strictly valid under the following conditions: constant concentration of the diffusing component at the particle surface, constant particle size and constant diffusion coefficient (diffusivity). In deriving a correction for varying diffusion coefficient, therefore, corrections to variable surface concentration and particle size may be implicit, depending on the scenario. Thus in the results below, the derivation of a correction is first studied for the relatively simple case of a constant surface mole fraction (determined through equilibration with a constant gas-phase saturation ratio). Second, the case of variable surface mole fraction (due to equilibration with a variable gas-phase saturation ratio) is studied. In addition, the effects of composition-dependent diffusion on number size distribution are demonstrated.

2 Method

In the first part of the method the model setup will be described, including all assumptions made. A simple two component system was assumed, comprising one semi-volatile (sv) and one non-volatile component (nv) that were nonreactive. Both components were assigned a molecular weight of 100 g mol^{-1} and a density of 1x10^{6} g m^{-3} (in the discussion it is shown that the model is sensitive to the ratio of the component molar volumes rather than absolute values of molecular weight or density). Ideality was assumed, therefore particle-phase volume was calculated by the addition of the product of each components' number of moles and molar volume. The initial particle-phase concentration was radially homogenous. For the purpose of deriving a solution to particle-phase diffusion independent of gas-phase diffusion the latter was assumed instantaneous. Therefore, in combination with the assumption of ideality, changes to the particle-phase surface mole fraction of the partitioning component implies equal changes to its gas-phase saturation ratio.

Fick's second law was solved by a numerical method; for a sphere, with spherical coordinates and with the diffusion coefficient (D) dependent on composition, this is (Crank, 1975):

$$\frac{\partial C_i(r,t)}{\partial t} = \frac{1}{r^2}\frac{\partial}{\partial r}\left(r^2 D_i(C_i)\frac{\partial C_i(r,t)}{\partial r}\right), \tag{1}$$

for component i, where C is concentration, r is radius and t represents time. In this study D followed a logarithmic dependence on the mole fraction of the semi-volatile component :

$$D(x_{sv}) = (D^0_{sv})^{x_{sv}}(D^0_{nv})^{(1-x_{sv})}, \tag{2}$$

where D^0 is the self-diffusion coefficient and x is mole fraction. This equation fitted measurements reported in Vignes (1966) for ideal mixtures. The model described below uses a stationary coordinate reference frame, which for an ideal binary system requires that each component have the same diffusivity, quantified by the diffusion coefficient. This is true regardless of the component molecular size, and is physically necessary to attain volume continuity (Taylor and Krishna, 1993; Krishna and Wesselingh, 199 The mathematical proof for the necessity of symmetric diffusion coefficients in an ideal binary system (e.g. comprising components 1 and 2) begins with:

$$\frac{-\nabla C_1}{\nabla C_2} = \frac{V_{m,2}}{V_{m,1}}, \tag{3}$$

where V_m is the molar volume and ∇C is the concentration gradient at the boundary where flux is being considered. Next, Fick's first law (which is equivalent to Fick's second law when flux is at steady state) can be expressed in terms of volumetric flux ($\mathrm{m^3\,s^{-1}}$):

$$J_i = D_i \nabla C_i V_{m,i} A, \tag{4}$$

where A is the area diffusion occurs over. The magnitude of volumetric flux has to be equivalent for both components in order to attain volume continuity. For a particle of finite volume this means mass continuity is also satisfied. With this stipulation and eq. 3, it can be seen that symmetric diffusion coefficients are physically necessary.

Equation 1 can be solved by several numerical methods (e.g. Zobrist et al., 2011; Shiraiwa et al., 2012), but here we use the initial-boundary problem approach (Fi-PaD) as presented in O'Meara et al. (2016). This model operates by splitting the particle into concentric shells, each assumed to be homogeneously mixed. The shell representation allows the radial profile of concentration (C) and therefore diffusion coefficient (D) to be realised. Increased steepness of the D gradient requires increased spatial resolution for accurate diffusion estimation. The volume of shells is revalued after every time step. Greater model temporal resolution is required with increased rates of volume change to account for the effect of particle size on diffusion rate. Therefore, as described in O'Meara et al. (2016), a maximum radius change of 0.1% was allowed over a single time step, and the interval was iteratively shortened until this condition was met.

The analytical solution to diffusion is presented and described in Zaveri et al. (2014). For a non-reactive component with instantaneous gas-particle surface equilibration it is:

$$\frac{d\overline{C}_{a,i,m}}{dt} = 4\pi R_{\mathrm{p},m}^2 N_m K_{p,i,m}(\overline{C}_{g,i} - \overline{C}_{a,i,m} S_{i,m}), \tag{5}$$

where $K_{p,i,m}$ is the overall mass transfer coefficient:

$$\frac{1}{K_{p,i,m}} = \frac{R_{p,m}}{5D_i}\left(\frac{C_{g,i}^*}{\sum_j \overline{C}_{a,j,m}}\right), \tag{6}$$

and $S_{i,m}$ is the saturation ratio:

$$S_{i,m} = \frac{C_{g,i}^*}{\sum_j \overline{C}_{a,j,m}}, \tag{7}$$

where $_a$ ~~and $_s$ represent the bulk and surface~~ represents the bulk of the particle-phase, ~~respectively,~~ $_g$ represents the gas-phase, j is the index for all components, m is the index for size-bin, R_p is particle radius, C_g^* is the effective saturation vapour concentration $(\mathrm{mol\,m^{-3}(air)})$, ~~$\overline{C}$ represents~~ $\overline{C}$ is the concentration in the bulk part of a phase $(\mathrm{mol\,m^{-3}(air)})$ and N is the particle number concentration $(\mathrm{m^{-3}(air)})$. In order to compare results from eq. 1 and eq. 5, concentrations from the latter must be divided by the volume concentration of particles $(\mathrm{m^3(particle)\,m^{-3}(air)})$. Following this division, it can be seen that diffusion has an inverse square dependence on particle radius in both solutions.

The analytical solution treats the particle as a single body, i.e., it cannot resolve radial heterogeneity of concentration and therefore diffusion coefficient (the $D-r$ profile). In order for the diffusion coefficient in the analytical method to respond to composition variation therefore, D was determined using eq. 2, which in turn used the bulk particle semi-volatile mole fraction ($x_{a,sv}$). Because D and the correction factor (derivation described below) varied with composition, the analytical solution was sensitive to temporal resolution. Analytical estimates were compared for a given scenario when the time steps of the Fi-PaD simulation were used and when a temporal resolution twice as fine was used. Results were identical, therefore the Fi-PaD resolution was considered sufficient for reliable analytical results.

Particles were assumed to initially have a radially homogenous concentration profile. Diffusion was then initiated by a change to the semi-volatile mole fraction at the particle surface ($\Delta x_{s,sv}$) to attain the equilibrium mole fraction $x_{s,sv,eq}$. The radial heterogeneity of D (in Fi-PaD) was therefore established through the setting of D_{sv}^0 and D_{nv}^0 and through the radial concentration gradient of the semi-volatile component resulting from diffusion. Since diffusion approaches equilibrium asymptotically, it is necessary to define an effective equilibrium point prior to complete equilibrium. We chose the e-folding state, which is when the absolute difference in component concentration at the surface and the bulk average (everything below the surface) decreases by a factor ~~or~~ of e from its initial value.

Fi-PaD estimates of the time required to reach the e-folding state (the e-folding time (t_e)) converged as its spatial resolution increased (O'Meara et al., 2016). The spatial resolution required to attain a satisfactory degree of convergence increased with

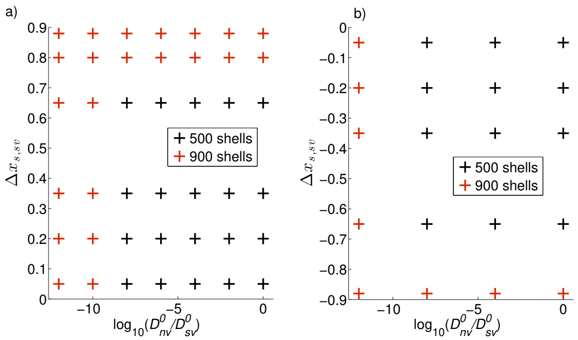

Figure 1. The shell resolution (given in the legend) distribution with $\Delta x_{s,sv}$ and $\log_{10}({}^{D^0_{nv}}/_{D^0_{sv}})$ used, for: a) positive (+ve) $\Delta x_{s,sv}$ and b) negative (-ve) $\Delta x_{s,sv}$.

the gradient of the $D-r$ profile, which in turn was proportional to $\Delta x_{s,sv}$ and ${}^{D^0_{nv}}/_{D^0_{sv}}$. The maximum acceptable change for *e*-folding time following the addition of a further shell was set at 0.1 %. Based on this condition, fig. 1 shows the shell resolution used for combinations of $\Delta x_{s,sv}$ and $\log_{10}({}^{D^0_{nv}}/_{D^0_{sv}})$. The majority of scenarios used a conservative shell resolution, and only where $|\Delta x_{s,sv}|$ and $|\log_{10}({}^{D^0_{nv}}/_{D^0_{sv}})|$ are both at a maximum for a given resolution was the convergence criteria neared.

As mentioned in the introduction, the correction of the analytical solution was for variation of not only the diffusion coefficient, but also particle size and surface concentration of the diffusing component. Consequently, corrections were derived and assessed for three scenarios of increasing complexity and generality. In the list of these scenarios below, the assumptions of ideality and instantaneous gas-phase diffusion mean that the condition of the surface mole fraction of the semi-volatile component also represents that of its gas-phase saturation ratio:

i) constant $x_{s,sv,eq}$, with initial/equilibrium $x_{s,sv}=0$ for positive (+ve, i.e. condensing case) $\Delta x_{s,sv}$/ negative (−ve, i.e. evaporating case) $\Delta x_{s,sv}$

ii) constant $x_{s,sv,eq}$, with initial/equilibrium $x_{s,sv}\neq 0$ for +ve $\Delta x_{s,sv}$/−ve $\Delta x_{s,sv}$

iii) variable $x_{s,sv,eq}$

For all scenarios the shell resolution distributions in fig. 1 were used to estimate the appropriate Fi-PaD spatial resolutions. To derive correction equations $R_\mathrm{p}-t$ profiles estimated by the analytical solution were fit ~~by eye~~ to those of Fi-PaD~~to derive correction equations~~. A least squares fitting procedure was attempted and found to be unconstrained, thus fitting was done by eye, and the quality of fit was objectively assessed through residuals, as described below. $\Delta x_{s,sv}$ and $\log_{10}({}^{D^0_{nv}}/_{D^0_{sv}})$ values across the ranges shown in fig. 1 were used, and the specific combinations shown in fig. 1 were used for the simplest derivation scenario (i) above). The analytical solution was found to have greater disagreement with the numerical solution for the condensation case than the evaporation case. Consequently fits were found for more combinations of $\Delta x_{s,sv}$ and $\log_{10}({}^{D^0_{nv}}/_{D^0_{sv}})$ for the condensation case, as shown in fig. 1. An interpolation method was developed to estimate parameters for the correction equation between the values of $\Delta x_{s,sv}$ and $\log_{10}({}^{D^0_{nv}}/_{D^0_{sv}})$ used for the equation derivation.

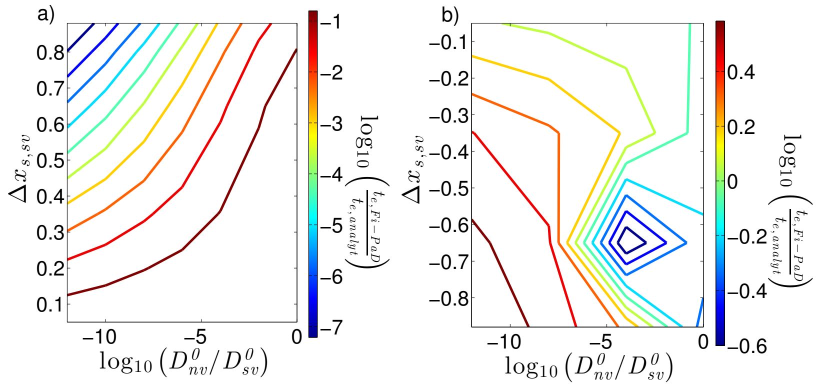

Figure 2. Ratio of Fi-PaD and analytical ($analyt$) estimated *e*-folding times (t_e) for: a) +ve $\Delta x_{s,sv}$ and b) -ve $\Delta x_{s,sv}$.

Finally, the following were incorporated into the Model for Simulating Aerosol Interactions and Chemistry (MOSAIC) (Zaveri et al., 2014): eq. 2, the correction equations and the interpolation method (eqs. 5-7 were already implemented). The temporal evolution of number size distributions was found for the case of condensation of a plasticiser and compared against an assumption of constant diffusivity. For elucidation of the effect on number size distribution of composition-dependent diffusion only the processes of gas/particle partitioning and particle-phase diffusion were modelled in MOSAIC.

3 Results

To begin, uncorrected analytical and Fi-PaD estimates of *e*-folding times were compared when D was dependent on composition (eq. 2). Estimates were made for the $\Delta x_{s,sv}$ and $\log_{10}(^{D^0_{nv}}/_{D^0_{sv}})$ combinations in fig. 1, and the discrepancy is shown in fig. 2. For the case of +ve $\Delta x_{s,sv}$ (condensation) (fig. 2a), the analytical solution tends to underestimate diffusion rate, a result of being unable to resolve the plasticising effect of the semi-volatile component as it diffuses inward. Consequently, the discrepancy increases with increasing values of $|\Delta x_{s,sv}|$ and $|^{D^0_{nv}}/_{D^0_{sv}}|$, which together determine the plasticising effect. For -ve $\Delta x_{s,sv}$ (evaporation) (fig. 2b), this trend is reversed for comparatively high values of $|\Delta x_{s,sv}|$ and $|^{D^0_{nv}}/_{D^0_{sv}}|$ because the analytical solution is unable to resolve the solidifying effect of the non-volatile component as the semi-volatile component diffuses outward. The solidifying effect decreases with decreasing $|\Delta x_{s,sv}|$ and $|^{D^0_{nv}}/_{D^0_{sv}}|$, whereas the inaccuracy introduced to the analytical by changing particle size is unaffected by $|^{D^0_{nv}}/_{D^0_{sv}}|$, but increases with $|\Delta x_{s,sv}|$. The competing effects of these sources of inaccuracy produce the irregular contour layout at higher values of $|^{D^0_{nv}}/_{D^0_{sv}}|$.

Generally the analytical solution is much more accurate for -ve $\Delta x_{s,sv}$, reaching a maximum absolute disagreement around 0.6 orders of magnitude compared to 7.0 for +ve $\Delta x_{s,sv}$. This is attributed to the different characteristics of diffusion between the -ve and +ve $\Delta x_{s,sv}$ cases. In the former, diffusion in Fi-PaD is limited by D near the particle surface, with a surface shell acting like a “crust”. During early stages, the plasticising effect of the semi-volatile component on this “crust” leads to comparatively rapid diffusion out of the particle, but the strength of this effect decreases with concentration of the semi-volatile component, so that the majority of the e-folding time is characterised by a gradual, relatively slow diffusion outward (see appendix for an example of the diffusion coefficient variation with radius for the evaporating case). The inability of the analytical solution to resolve the limiting diffusion near the surface leads to a greater rate of initial diffusion, however the consequent decrease in semi-volatile component concentration results in a D value that replicates the slow diffusion phase of Fi-PaD. In contrast, for +ve $\Delta x_{s,sv}$, diffusion is limited at the diffusion “front~~"~~”, which is the shell boundary between shells with the greatest radial gradient of concentration. Modelling movement of the “front~~"~~” requires knowledge of the concentration gradient there, however the only information available to the analytical approach is the particle bulk concentration, leading to the large discrepancies seen.

To bring the analytical and numerical solutions into agreement, a correction factor is proposed for the analytical solution. This will act on the diffusion coefficient to correct the diffusion rate (and is therefore denoted by C_D). Eq. 6 is thus modified to:

$$\frac{1}{K_{p,i,m}} = \frac{R_{p,m}}{5C_D D_i}\left(\frac{C^*_{g,i}}{\sum_j \overline{C}_{a,j,m}}\right). \tag{8}$$

To derive a function for C_D first the simplest scenario of a single and instantaneous change in $x_{s,sv}$ with the initial/final $x_{s,sv} = 0$ for +ve $\Delta x_{s,sv}$/-ve $\Delta x_{s,sv}$ is investigated. The correction factor for D required to bring analytical R_p estimates into agreement with those of Fi-PaD was found at each time step used by the latter model. The correction factor was then plotted against ~~a metric for~~ proximity to equilibrium; ~~for +ve $\Delta x_{s,sv}$ this was the ratio of surface to bulk average x_{sv}, while for -ve $\Delta x_{s,sv}$, this was the~~ here we use the absolute difference between surface and bulk average x_{sv}. This process was done for the model inputs shown in fig. 1 to determine whether a general equation form could be found that described the relationship between the D correction factor (C_D) and proximity to equilibrium. Examples are shown in fig. 3. The resulting general ~~equations for~~ equation for both +ve and -ve $\Delta x_{s,sv}$ ~~, respectively, are~~ is found to be:

$$C_D = \left(e^{(-(x_{s,sv}/x_{a,sv}-p_1)^{p_2})/p_3} + p_4\right)^{-1((|x_{s,sv}-x_{a,sv}|)^{p_1})p_2} - p_3, \tag{9}$$

~~and~~

$$C_D = e^{((x_{a,sv}-x_{s,sv})^{p_1})p_2} - p_3,$$

where p_n is a parameter value, dependent on $\Delta x_{s,sv}$ ~~(the change in semi-volatile surface mole fraction from the initial value (equal to the initial bulk particle mole fraction)) and~~ and ${}^{D^0_{nv}}/{}_{D^0_{sv}}$. Where the self diffusion coefficients of components are the same in fig. 3, the correction is required only for the changing particle size. Oscillations in C_D occur for the case of $\Delta x_{s,sv} = -0.88$ and $\log_{10}({}^{D^0_{nv}}/{}_{D^0_{sv}}) = -12$. This is attributed to the competing effects of changing particle size, which for a shrinking particle, acts to overestimate diffusion rate, and of a composition-dependent D, which for a solidifying particle acts to underestimate diffusion time. As diffusion proceeds, slight variations in the relative strengths of these effects causes C_D to oscillate. Nevertheless, an overall trend is discernible and can be described by eq. 9.

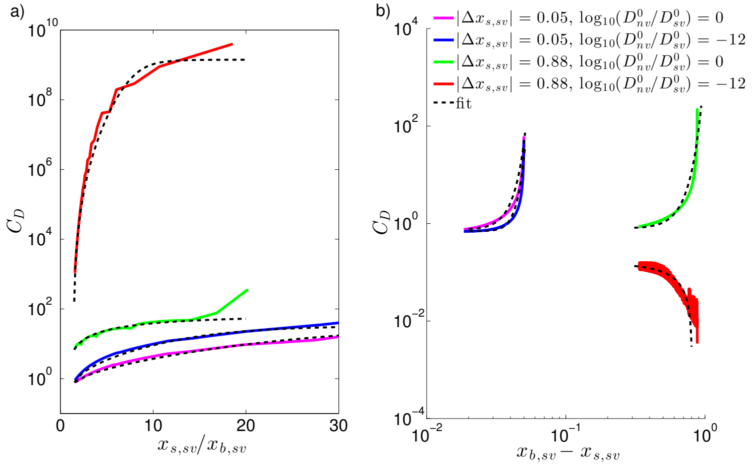

Figure 3. Examples of the correction factor for D in the analytical solution (C_D) required to give agreement with radius estimates in Fi-PaD as a function of proximity to equilibrium~~(for which the metric depends on the sign of $\Delta x_{s,sv}$), for: ~~. a) and b) are for +ve $\Delta x_{s,sv}$ and ~~b) ~~-ve $\Delta x_{s,sv}$, respectively. The model scenario is described in the legend, which applies to both plots. Fits are plotted using ~~eqs~~eq. ~~?? and ~~9~~for a) and b), respectively~~.

Parameter values for ~~eqs. ?? and ~~eq. 9 were found through fitting ~~by eye ~~analytical $R_\mathrm{p} - t$ profiles with those of Fi-PaD for the model inputs shown in fig. 1 (values are provided in the appendix). To ~~value the agreement between Fi-PaD and corrected analytical estimates~~objectively test the goodness of fit, the following equation was used:

$$\%\quad \text{error} = \left(\frac{R_{\mathrm{p},Fi-PaD,t} - R_{\mathrm{p},analyt,t}}{|R_{\mathrm{p},Fi-PaD,t=t_e} - R_{\mathrm{p},Fi-PaD,t=0}|}\right)100, \tag{10}$$

where $analyt$ represents the corrected analytical model. Therefore, $\%$ error is the fraction of the total change in R_p comprised by the disagreement in model estimates of R_p at t.

For each marked $\Delta x_{s,sv}$ value in fig. 1, the marked $\log_{10}(^{D^0_{nv}}/_{D^0_{sv}})$ scenario with greatest $\%$ error was identified. Of these scenarios, the four with greatest $\%$ error are shown in fig. 4 to demonstrate the cases of worst agreement. Fig. 4 shows that the disagreement between analytical and Fi-PaD model estimates rarely exceeds ±6%, even for cases representing the extremes of model disagreement. Corrected analytical and numerical solution results were also compared beyond the e-fold time, until the difference in concentration between surface and bulk had diminished to a factor of $16e$. The agreement shown in fig. 4 was maintained to this further equilibration point.

In order to have general applicability, such good agreement must be reproducible for intermediate values of $\Delta x_{s,sv}$ and $\log_{10}(^{D^0_{nv}}/_{D^0_{sv}})$, i.e., when parameter values are interpolated between the points of fig. 1. Parameter relationships with $\Delta x_{s,sv}$ and $^{D^0_{nv}}/_{D^0_{sv}}$ varied substantially, requiring separate interpolation methods for each parameter. The ~~interpolation methods are~~

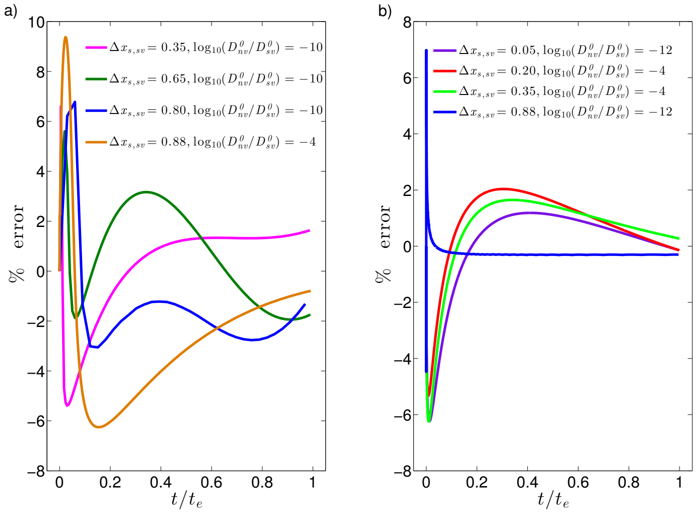

Figure 4. Examples of $\%$ error (eq. 10) of the analytical model with corrected D when diffusion is composition-dependent (eq. 2), plotted against time normalised by the e-folding time. a) and b) are for +ve $\Delta x_{s,sv}$ and -ve $\Delta x_{s,sv}$, respectively, and scenarios are given in the legend.

~~presented~~ general method was to first interpolate with respect to $\Delta x_{s,sv}$ followed by $^{D^0_{nv}}/_{D^0_{sv}}$. For most accurate results the interpolation equation was found to be dependent on the independent variables as described in the appendix ~~and were~~ (table A3 and table A4). The interpolation was tested at $\Delta x_{s,sv}$ and ~~$\log_{10}(^{D^0_{nv}}/_{D^0_{sv}})$~~ $^{D^0_{nv}}/_{D^0_{sv}}$ comparatively far from those with known parameter values and spread across the variable space. Results are shown in fig. 5, again using the $\%$ error metric presented in eq. 10. They show that the low error produced for known parameter values is maintained when the interpolation method is applied.

Next, the case of a single and instantaneous change to $x_{s,sv}$ with the initial/final $x_{s,sv} \neq 0$ for $+$ve $\Delta x_{s,sv}$/$-$ve $\Delta x_{s,sv}$ is studied. For the $+$ve $\Delta x_{s,sv}$ case, the correction method described above was found to be transferable to any starting $x_{s,sv}$ through transformation of the D dependence on x_{sv}. An effective self-diffusion coefficient of nv ($D^0_{nv,eff}$) is set as the D at the starting $x_{s,sv}$ (eq. 2), and the starting $x_{s,sv}$ for the analytical is set to 0. D^0_{sv} is constant, but the equilibrium $x_{s,sv}$ ($x_{s,sv,eq}$) is changed to an effective value such that D at equilibrium gives the same change in D from the starting $x_{s,sv}$ as in the original scenario. Consistent with eq. 2 this effective $x_{s,sv,eq}$ is given by:

$$x_{s,sv,eq,eff} = \frac{(\log_{D^0_{nv,eff}}((D^0_{nv})^{(1-x_{s,sv,eq})}(D^0_{sv})^{(x_{s,sv,eq})}) - 1)}{(\log_{D^0_{nv,eff}}(D^0_{sv}) - 1)}, \tag{11}$$

where $x_{s,sv,eq}$ and D^0_{nv} are the original values. An example transformation to this effective model setup is shown in fig. 6. It can be seen that, compared to the original setup, $\Delta x_{s,sv}$ is increased. Although the transformed D gradient with $x_{s,sv}$ is shallower than the original, ~~therefore,~~ this is offset in terms of diffusion rate by the increased radial gradient in sv concentration.

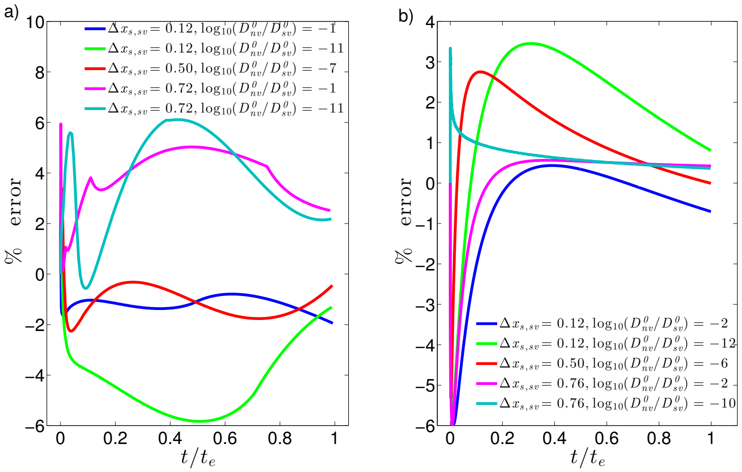

Figure 5. Examples of $\%$ error (eq. 10) of the analytical model with corrected D and composition-dependent on diffusion (eq. 2), plotted against time normalised by the e-folding time. Parameter values for ~~eqs~~eq. ~~?? and~~ 9 were found through the interpolation method presented in the appendix (Tables A3 and A4). a) and b) are for +ve $\Delta x_{s,sv}$ and -ve $\Delta x_{s,sv}$, respectively, and model setups are given in the legend.

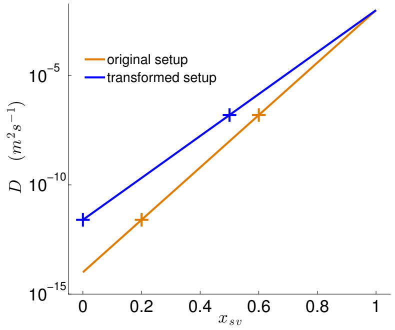

Figure 6. Example of the transformation of the D dependence on x_{sv} when the starting $x_{s,sv}$ (for condensation) or final $x_{s,sv}$ (for evaporation) $\neq 0$. In this example the original starting $x_{s,sv}$ was 0.2 and the equilibrium $x_{s,sv}$ was 0.6, while the original D^0_{nv} was 1x10^{-14} m^{2}s^{-1} and D^0_{sv} was 1x10^{-2} m^{2}s^{-1}, as shown by the orange crosses. The effective starting and equilibrium $x_{s,sv}$ and effective D^0_{nv} found by the transformation described in the main text are shown with blue crosses.

A similar method can be applied to the evaporation scenario when the final $x_{s,sv} \neq 0$. $D^0_{nv,eff}$ is set equal to that at the final $x_{s,sv}$, and the final $x_{s,sv}$ is set to 0. Whereas for the +ve $\Delta x_{s,sv}$ case we found $x_{s,sv,eq,eff}$, now an effective start $x_{s,sv}$ ($x_{s,sv,0,eff}$) is required. The equation for this is the same as eq. 11, but with $x_{s,sv,eq,eff}$ replaced by $x_{s,sv,0,eff}$ and with $x_{s,sv,eq}$ replaced by $x_{s,sv,0}$. With regard to the transformed $D - x_{sv}$ profile (e.g. fig. 6), for a given pair of original start and finish $x_{s,sv}$ and a given pair of original self-diffusion coefficients, the transformation is the same for +ve and -ve $\Delta x_{s,sv}$.

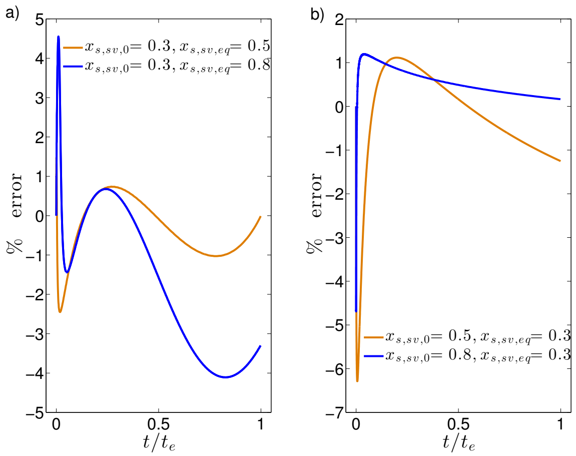

Figure 7. Agreement between corrected analytical and Fi-PaD estimates, using the metric given in eq. 10, for: a) +ve $\Delta x_{s,sv}$ and b) -ve $\Delta x_{s,sv}$, as shown in the legend. The start/finish $x_{s,sv} \neq 0$ for a)/b), therefore the transformation to an effective model setup (as described in the main text) was required. For both a) and b) $\log_{10}(^{D^0_{nv}}/_{D^0_{sv}}) = -12$.

To exemplify the deviation in analytical (with correction) estimates of diffusion rate from those of Fi-PaD when this transformation is applied, the cases of $\Delta x_{s,sv} = 0.2$ and $= 0.5$, and a comparatively large $\log_{10}(^{D^0_{nv}}/_{D^0_{sv}})$ of -12 were used. Estimates were compared using eq. 10. Results for +ve and -ve $\Delta x_{s,sv}$ are given in fig. 7, and demonstrate that the deviations are comparable to those when the transformation is not required (fig. 4).

Before moving onto a correction for the case of variable $x_{s,sv}$, the correction for constant $x_{s,sv}$ was implemented in MOSAIC to investigate the effect of composition-dependent diffusion on number size distribution. The same initial number size distribution as presented in Zaveri et al. (2014) (their fig. 11) was used. Reactions, coagulation, nucleation, emission and deposition were all turned off to gain the clearest demonstration of the diffusion effect. To maintain $x_{s,sv}$, the gas-phase concentration of the semi-volatile component was held constant and low particle-phase self-diffusion coefficients were used to ensure that partitioning was not limited by diffusion in the vapour-phase. The model was run in Langrangian mode to prevent numerical error due to rebinning and resultant loss of information about the initial particle size.

To test the effect on the timescale of number size distribution change during condensation of a plasticising semi-volatile component, $\Delta x_{s,sv}$ was set to +0.88, from an initial particle-phase mole fraction of 0. The number size distribution following diffusion was found for $\log_{10}(^{D^0_{nv}}/_{D^0_{sv}})$ values of 0, -2 and -4, with D^0_{nv} held constant at $1.0\text{x}10^{-26}$ m^2s^{-1}. Simulations were run until ~~the largest particle had reached its e-folding state~~diffusion was underway in large particles. The distributions after one ~~tenth~~ hundredth and at the end of the run time (1.2x10^8 s) for the $\log_{10}(^{D^0_{nv}}/_{D^0_{sv}})$=-4 case are shown in fig. 8a and fig. 8b, respectively, along with the initial distribution.

As expected, fig. 8 shows that the condensing component can significantly increase the rate of diffusion and therefore the rate at which the number size distribution evolves. ~~For all values of $\log_{10}(^{D^0_{nv}}/_{D^0_{sv}})$ the form of the~~ The development of the number

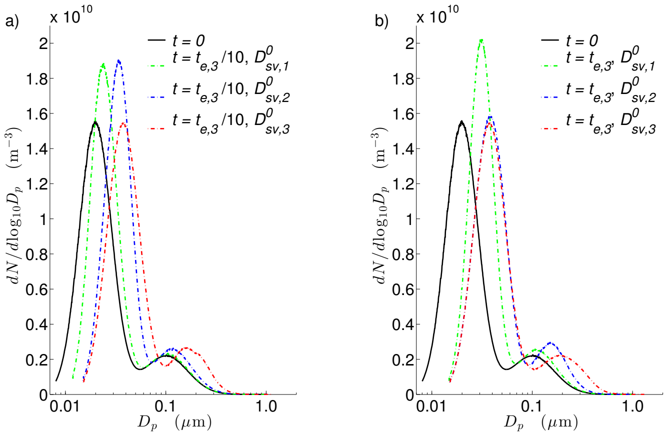

Figure 8. Number size distributions for $\log_{10}(D^0_{nv}/D^0_{sv})$ = 0, -2 and -4, represented by $D^0_{sv,1}$, $D^0_{sv,2}$ and $D^0_{sv,3}$ respectively (D^0_{nv} constant at $1.0\text{x}10^{-26}$ m^2s^{-1}). $t_{e,3}$ is ~~the time for the largest particle in the $\log_{10}(D^0_{nv}/D^0_{sv})$ = -4 run to attain e-folding state~~1.2x10^8 s. a) is the distribution at one tenth of $t_{e,3}$ and b) is that at $t_{e,3}$. $x_{s,sv}$ was increased instantaneously from 0.00 to 0.88 and then held constant.

size distribution shows ~~the same characteristic of initially narrowing as smaller particles grow more quickly before widening again as these~~ no dependence on $\log_{10}(D^0_{nv}/D^0_{sv})$ since any change in the plasticising strength of the condensate effects the same factor change in diffusion rate for all particle sizes . For each self-diffusion coefficient ratio there is preferential growth of smaller particles first due to the square dependence of diffusion rate on particle radius, leading to a narrowing of the distribution. This is followed by a widening as smaller particles equilibrate and larger particles grow ~~. The degree of narrowing is similar between all cases, indicating that when a plasticising effect occurs, the resulting acceleration of diffusion is similar across all particle sizes~~ (consistent with ~~the results of O'Meara et al. (2016)~~Zaveri et al. (2014)).

It is possible to set a constant diffusion coefficient in the analytical solution without correction that attains the same e-folding time as when the analytical solution with correction is used with a variable diffusion coefficient. For the case of $D^0_{nv} = 1.0\text{x}10^{-26}$ and $D^0_{sv} = 1.0\text{x}10^{-22}$ m^2s^{-1} and $\Delta x_{s,sv} = 0.88$, the required constant diffusion coefficient was found to be $D_{con} = 4.4\text{x}10^{-23}$ m^2s^{-1}. The % error (eq. 10) when the constant D treatment ~~is~~ and the corrected analytical solution are used is shown in fig. 9a. This figure shows that although the constant D simulation does give the same e-fold time (agreement in radius estimate at $t/t_e = 1$), diffusion estimates about this point are different between the treatments of diffusion coefficient~~: beginning more quickly in the variable casebefore it slows~~. In the constant case, slower diffusion relative to the ~~constant case~~numerical solution and corrected analytical solution is initially estimated, followed by quicker diffusion after e-fold time.

To test the effect of using a constant D on a polydisperse population, this treatment is used to estimate number size distributions from MOSAIC and compared to estimates using the variable D treatment. Using the same model setup as for fig. 8, the comparison is shown in fig. 9b-d . Results are shown for three times since run start as described in the figure. As expected from fig. 9a, if one focusses on the smaller particle sizes it can be seen that growth is initially quickest in the variable D case (fig. 9b) but that growth in the constant D case catches and exceeds that for variable D, leading to increased narrowing of

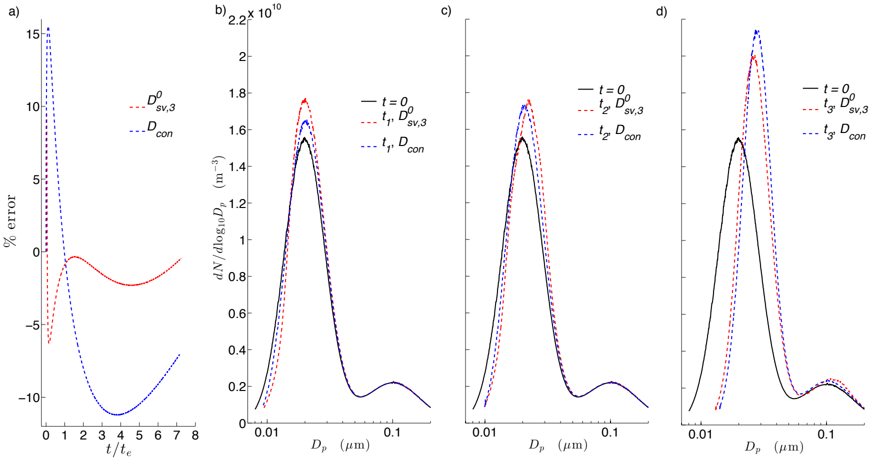

Figure 9. In a), the discrepancy (found using eq. 10) in estimated radius with model run time normalised to the e-folding time (t_e) when $x_{s,sv}$ is increased instantaneously from 0.00 to 0.88 for two diffusion coefficient treatments: i) corrected analytical solution with $D^0_{nv} = 1$x10^{-26} and $D^0_{sv} = 1$x10^{-22} m^{2}s^{-1} ($D^0_{sv,3}$) and ii) using the analytical without correction when D is constant at 4.4x10^{-23} m^{2}s^{-1} (D_{con}). In later plots are the number size distributions for the same diffusion coefficient treatments, with red representing the former treatment (variable D) and blue the latter one (constant D)). In b) ~~$t = 1.80$x10^4~~ $t = 2.4$x10^4 s, c) ~~$t = 4.50$x10^4~~ $t = 4.8$x10^4 s and in d) ~~$t = 5.76$x10^5~~ $t = 1.2$x10^5 s since simulation start.

the distribution (fig. 9d). Note that while this demonstration focuses on the smallest sizes, the same effect is true for all sizes~~, indeed in fig. 9d for D_p around 0.1 μm it can be seen that particles are growing quicker in the variable treatment as diffusion initiates in these sizes.~~. These discrepancies demonstrate the requirement for a correction to the analytical solution that is dependent on the proximity to equilibrium rather than a correction based on a constant D.

For the analytical solution to be generally applicable a correction when $x_{s,sv}$ varies prior to particle phase equilibration is required. If the rate of $x_{s,sv}$ change is very low compared to particle-phase diffusion (particle-phase equilibration reached with negligible change of $x_{s,sv}$), or very high compared to particle-phase diffusion (no diffusion in the particle-phase before the surface concentration reaches a constant value), no correction is needed. In between, however, a further correction dependent on the rate of $x_{s,sv}$ change is required. Changes to $x_{s,sv}$ may result from changes to the saturation ratio of the semi-volatile component. This may occur through a variety of ways, but in general is due to the sum of emission and production being different to that of deposition and destruction. Processes controlling gas-phase component concentrations occur at rates varying by several orders of magnitude (e.g. reaction rate with OH radicals (Ziemann and Atkinson, 2012)). The rate of particle-phase diffusion may also vary by orders of magnitude, as it is dependent on the concentration and diffusivity of the diffusant as well as the diffusivity of the initial particle and the particle size (O'Meara et al., 2016).

Results shown to this point have been for a constant $x_{s,sv}$ (implying instantaneous particle surface-gas equilibration and a constant gas phase saturation ratio). Application of the ~~corrections~~ correction presented above (~~eqs. ?? and~~ eq. 9) to the variable case is not straightforward as it is based on the difference between initial and equilibrium mole fractions and the particle is assumed to initially have a radially homogenous concentration profile. In the following passage is a description of a method to overcome this constraint for a given time profile of $x_{s,sv}$. This serves as a basis to explain the limits of this method to general application.

$x_{s,sv}$ was decreased from 0.88 to 0.00 with a sinusoidal profile, as shown in fig. 10a (curve ~~p_1~~prof_1). The initial particle radius was 1x10^{-4} m, $D^0_{nv} =$ 1x10^{-14} and $D^0_{sv} =$ 1x10^{-10} m^{2}s^{-1}. The resulting $R_\mathrm{p} - t$ profile using Fi-PaD is shown in fig. 10b. ~~For the analytical estimate to agree the correction equation is~~ A new correction equation was required that could accommodate a variable surface mole fraction and give agreement with Fi-PaD estimates. Through fitting by eye this was found to be:

$$C_D = e^{((p_4)^{p_1})p_2} - p_3, \tag{12}$$

where

$$p_4 = \frac{x_{a,sv}}{(\sin(\log_{10}(x_{rat,t_n} - x_{rat,t_{n-1}})/1.3 - 2.4)/4.6 + 1.1)}, \tag{13}$$

where x_{rat} is the ratio of x_{sv} in the particle bulk to that at the surface. The ratios at the start of the time step being solved for (t_n) and at the start of the previous time step (t_{n-1}) are used. p_1, p_2 and p_3 are the same as used for the original equation (eq. 9) and $\Delta x_{s,sv}$ was set equal to the particle bulk x_{sv}.

This correction gives excellent agreement with the Fi-PaD estimate (fig. 10b). However, when used for a slightly different temporal profile of $x_{s,sv}$ (curve ~~p_2~~ prof_2 in fig. 10a), poorer agreement is attained. This indicates that the correction described in eqs. 12-13 is over fitted. This is unsurprising as it is dependent on the rate of change of the surface mole fraction of the semi-volatile component (through $x_{rat,tn} - x_{rat,tn-1}$). Consequently, we suggest that a generally applicable correction is only possible with an a priori estimate of the rate of change of bulk to surface mole fraction ratio. However, the bulk mole fraction is the value being estimated, making a solution intractable using this methodology.

Also shown in fig. 10 is the expected range in rate of change of particle surface mole fraction of a semi-volatile component assumed to be in equilibrium with the gas-phase due to three processes: chemical reaction, dry deposition and condensation onto particles. The rates of change cover several orders of magnitude depending on the rate constants (given in the caption). Comparing these rates to the e-folding times for particle phase diffusion given in O'Meara et al. (2016), it is clear that under certain scenarios the surface mole fraction change rate is similar to particle-phase diffusion rate. In this instance, the corrections presented above break down. In contrast, when the particle-phase diffusion rate is much slower than the change in surface mole fraction of semi-volatile, a constant surface mole fraction may be assumed and the correction applied with the high accuracy presented above. This scenario is more likely to arise for particles with low diffusivity, and therefore of interest to particle-phase diffusion studies.

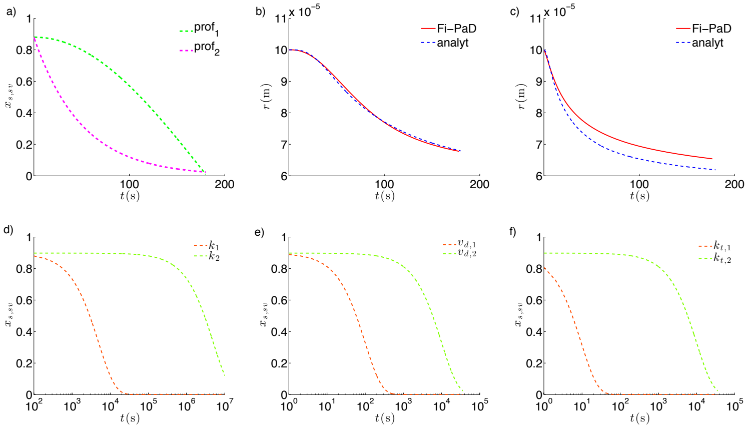

Figure 10. Plots demonstrating the limitation of the correction to cases of varying $x_{s,sv}$. In a) are the two temporal profiles of $x_{s,sv}$ used to test accuracy, while b) and c) show Fi-PaD and analytical (analyt) estimates of radius (the latter corrected using eqs. 12 and 13) for $x_{s,sv}$ temporal profiles p_1 and p_2, respectively. $D^0_{nv} = 1\text{x}10^{-14}$ and $D^0_{sv} = 1\text{x}10^{-10}\ \mathrm{m^2s^{-1}}$. In the lower row of plots are the range in rates of surface mole fraction change of a semi-volatile component assuming instantaneous equilibration with the gas-phase due to three processes: d) gas-phase chemical reaction with OH, with $k_1 = 1.0\text{x}10^{-5}\,\mathrm{m^3\,molecule^{-1}\,s^{-1}}$ and $k_2 = 1.0\text{x}10^{-8}\,\mathrm{m^3\,molecule^{-1}\,s^{-1}}$ (Ziemann and Atkinson, 2012); e) dry deposition to land surface, with $v_{d,1} = 1.0\text{x}10^{-2}\,\mathrm{m\,s^{-1}}$ and $v_{d,2} = 1.0\text{x}10^{-4}\,\mathrm{m\,s^{-1}}$ (Sehmel, 1980); f) condensation onto particles, with $k_{t,1} = 1.0\text{x}10^{-1}\,\mathrm{s^{-1}}$ and $k_{t,2} = 1.0\text{x}10^{-4}\,\mathrm{s^{-1}}$ (Sellegri et al., 2005; Whitehead et al., 2012).

4 Discussion

As mentioned in the introduction, for a simple case of diffusion independent of composition, the computer time for the numerical solution is approximately 20 times as long as the analytical. However, this factor difference is expected to rise by 2-3 orders of magnitude for very steep gradients of diffusion coefficient with radius (O'Meara et al., 2016). Therefore, implementation of composition-dependent diffusion into a polydisperse multi-process aerosol model like MOSAIC through an analytical solution is highly preferable to a numerical one. Here, equilibration between the gas- and particle-phase was assumed instantaneous, so that the surface mole fraction of the partitioning component was equal to its gas-phase saturation ratio.

For the limiting case of constant surface mole fraction of a semi-volatile component, here a correction to the analytical solution for when diffusivity is composition-dependent has been derived and validated against estimates from the numerical solution. The correction was required to account not only for variable diffusivity but also varying particle size as the semi-volatile component partitions between phases, since the uncorrected analytical solution assumes constant particle size. A method to interpolate correction parameters between values of $\Delta x_{s,sv}$ (change to surface mole fraction that initiates diffusion) and $^{D^0_{nv}}/_{D^0_{sv}}$ (ratio of component self-diffusion coefficients) was also derived and validated. A similar derivation was attempted for the case of variable surface mole fraction, however this was found to be of narrow applicability. This issue, along with the limitations of the correction for constant $x_{s,sv}$ are discussed below.

In favour of the correction is its independence of particle size. In both solutions (numerical and analytical), diffusion rates have a square dependence on particle size, therefore the ratios of estimated diffusion rate are constant across sizes (all else being equal), as is the correction. Similarly, the correction is independent of absolute values of D^0_{nv} and D^0_{sv} and only dependent on the ratio of component self-diffusion coefficients: $\log_{10}({}^{D^0_{nv}}/{}_{D^0_{sv}})$.

Although the correction is applicable across particle sizes and values of D^0_{nv} and D^0_{sv}, it is specific to the ratio of component molar volumes used here, which is 1:1. The change in particle size due to partitioning depends on the molar volumes of components. The response of diffusion rate to a change in molar volume is different between the models and is non-linear in each. For quantifying model sensitivity to molar volume, a further complication is the variation of diffusivity with both molar mass and density (Koop et al., 2011).

To gain an indication of the model disagreement arising from changing molar volume when the corrected analytical model is used, expected ranges of molar mass (M) and density (ρ) for atmospheric organic components were found. Barley et al. (2011) show that M is likely to be in the range $1\text{x}10^2$ to $3\text{x}10^2$ g mol^{-1} and Topping et al. (2011) demonstrate that ρ is likely to be between $1.2\text{x}10^6$ to $1.6\text{x}10^6$ g m^{-3}. The maximum expected molar volume for the semi-volatile component was therefore given by using $\text{M} = 3\text{x}10^2$ g mol^{-1} and $\rho = 1.2\text{x}10^6$ g m^{-3}. A relatively large effect from the changed molar volume was gained through using $\Delta x_{s,sv} = \pm 0.88$. Furthermore, the proportion of the correction attributed to particle size change rather than D composition dependence, is greatest for $\log_{10}({}^{D^0_{nv}}/{}_{D^0_{sv}}) = 0$, therefore this was used to maximise the effect of varying molar volume on model agreement. For the +ve and -ve $\Delta x_{s,sv}$ cases, the maximum observed % error (eq. 10) was -58.0 and 29.0 %, respectively. Given this large discrepancy and the complexity of the model responses, we recommend further work to investigate correction dependence on molar volume. The presented correction parameters are therefore restricted to components with the same molar volume and are not applicable to cases where water diffuses through a particle comprising of a component(s) of substantially different molar volume. The organic components expected to significantly decrease particle-phase diffusivity have either long carbon backbones or are highly oxygenated and are therefore likely to have a molar volume several factors lower than water (Kroll and Seinfeld, 2008; Koop et al., 2011; Saukko et al., 2012; Ehn et al., 2014; Tröstl et al., 2016). Different parameters would be required for the presented correction equation (eq. 9) to be applicable to cases with components of variable molar volume.

A further limitation of the presented correction is its specificity to the D dependence on composition. Here we have assumed a logarithmic dependence on x_{sv}, however, measurements have reported sigmoidal and irregular dependencies resulting from changes to phase state and/or non-ideality (e.g. Vignes, 1966; Lienhard et al., 2014; Price et al., 2015). An indication of model disagreement generated by varying the D dependence was found by calculating the % error for several dependencies; all were based on a sigmoidal function, however, the steepness at the “cliff-edge~~"~~” was varied, as shown in fig. 11a. Also shown here is the logarithmic dependence used to find the presented correction. A $\log_{10}({}^{D^0_{nv}}/{}_{D^0_{sv}}) = -12$ and $\Delta x_{s,sv} = \pm 0.88$ were used because these provide the most stringent test of estimation capability. The dependencies were used in both the Fi-PaD and analytical model, with the latter using the correction method for the logarithmic dependence. The resulting discrepancies in estimated particle radius are shown in figs. 11b and 11c.

Fig. 11b shows that for +ve $\Delta x_{s,sv}$, the analytical method increasingly overestimates initial diffusion with increasing sigmoidal function steepness, indicating the correction is too great when the ~~ratio of surface to~~ difference in surface and bulk x_{sv} is high. The reason is that, with the dependencies used, increased steepness causes increased resistance to inward semi-volatile diffusion at low x_{sv}. As ~~surface to~~ the difference in surface and bulk x_{sv} ~~ratio~~ decreases in the analytical, so does the correction factor (fig. 3a), ~~and~~ allowing Fi-PaD estimates ~~begin to converge on the analytical~~ to approach those of the analytical (the upward part of curves). For the least steep sigmoidal dependence ~~, diffusion in~~ (sig1) this effect continues and Fi-PaD ~~overtakes the corrected analyticalaround 0.3 t/t_e. This occurs after some initial diffusion and is therefore attributed to~~ diffusion actually overtakes the analytical. For the intermediate sigmoidal profile (sig2) this effect occurs until the analytical system reaches a semi-volatile mole fraction where the profile curves sharply upward. Now the effect of increasing diffusion coefficient in the analytical surpasses the effect of a relatively small correction factor that had allowed Fi-PaD diffusion ~~occurring quickly~~ estimates to accelerate relative to the ~~logarithmic dependence once the bulk concentration of the semi-volatile has been raised. This is demonstrated in fig. 11a, where for the least steep sigmoidal dependence, above $x_{sv} \approx 0.3$ the same change in x_{sv} gives a greater increase in diffusivity than in the logarithmic dependence~~analytical, causing a relative acceleration of diffusion in the analytical. The result is the downward curve for the intermediate profile towards equilibrium time. The same process would arise for the steepest sigmoidal profile shown here (sig3) if sufficient diffusion occurred to allow the system to enter the mole fraction region where the diffusion coefficient curves upward.

Results for -ve $\Delta x_{s,sv}$ are shown in fig. 11c, which shows that the analytical solution initially underestimates diffusion. This is attributed to the increasing plasticising effect of the semi-volatile on the surface crust of the particle with increasing steepness of the sigmoidal “cliff-edge~~"~~”. Once x_{sv} has decreased however, the analytical shows a tendency to overestimate diffusion. The plasticising effect can quickly decrease (fig. 11a), and the surface crust imposes a greater impediment to diffusion. The correction factor (which acts to decelerate diffusion (fig. 3b)) found from the logarithmic dependence is insufficient to replicate this for the steepest dependency.

As fig. 11 shows, the presented correction is limited in its generality with regards to diffusion coefficient dependence on composition. Along with the effect of molar volume on diffusion, however, it is conceivable that this could be overcome through a more advanced correction similar in approach to that presented. In contrast, results indicate that improving the accuracy of the correction for the case of changing particle surface mole fraction is not attainable, since this requires a priori knowledge of the particle-phase diffusion rate (the value being estimated). Nevertheless, for studies into particle-phase diffusion limitation on particle transformation, it is possible that the surface mole fraction will vary quickly compared to particle-phase diffusion, allowing the assumption of a constant surface mole fraction and therefore accurate application of the correction presented here.

Without a general analytical solution (e.g. allowing for varying surface mole fraction), thorough evaluation of particle-phase diffusion influence on particulate transformation remains limited. The correction for constant surface mole fraction of the semi-volatile component, however, offers improved computer efficiency (compared to numerical methods) of evaluating particle-phase diffusion effects, such as in Berkemeier et al. (2013) and Mai et al. (2015). It may also be of use for the inference of diffusivity from laboratory studies, if the rates of semi-volatile gas-phase saturation ratio change and gas-phase diffusion are much greater than the particle-phase diffusion rate (Zobrist et al., 2011; Lienhard et al., 2014; Steimer et al., 2015). In

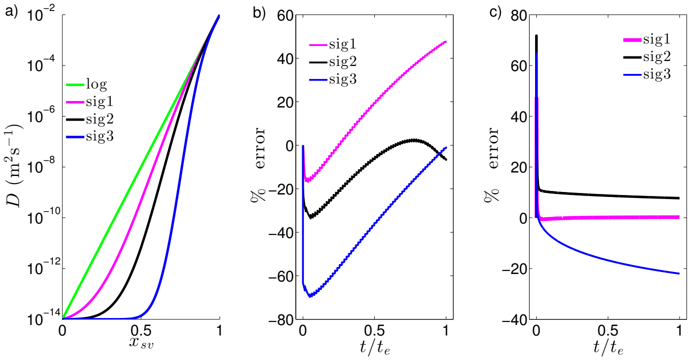

Figure 11. Plot a) shows the logarithmic dependency of diffusion coefficient on mole fraction on which the presented correction is derived and the sigmoidal dependencies for which it was tested. In b) and c) ~~is~~ are the analytical model ~~error~~ errors (eq. 10) when the sigmoidal dependencies given in a) were used. b) +ve $\Delta x_{s,sv}$ and c) -ve $\Delta x_{s,sv}$, and for both plots $|\Delta x_{s,sv}| = 0.88$ and $\log_{10}(D^{0}_{nv}/D^{0}_{sv}) = -12$.

modelling studies where composition-dependent diffusion occurs and gas-phase saturation ratios of partitioning components vary over similar timescales to particle-phase diffusion, we recommend the numerical solutions mentioned above in preference to the assumption of constant diffusivity.

5 Conclusions

For accurate simulation of the transformation of particulates containing organic components, the analytical solution to diffusion must account for composition-dependent diffusion rate. To do this, a correction to the analytical solution was investigated based on estimates from the numerical solution of the partial differential equation for diffusion. A correction was derived for the limiting case of a constant surface mole fraction of the diffusing component (equal to a constant gas-phase saturation ratio when assuming equilibration between the gas- and particle-phase). The corrected analytical solution shows good agreement with the numerical one, rarely exceeding 8 % deviation in estimated particle radius change.

The verified correction is currently limited to conditions of similar molar volume between the partitioning component and the particle average, and of a logarithmic dependence of diffusion coefficient on partitioning component mole fraction. These limitations may be overcome through an advanced correction. However, a correction for the more general case of variable surface mole fraction of the diffusing component (e.g., due to varying gas-phase saturation ratio) was found to depend on the rate of change of the ratio of bulk to surface mole fraction. A correction based on the analytical approach presented here is therefore not viable because it requires a priori knowledge of the value to be estimated: the particle bulk mole fraction. A different approach to modifying the analytical solution to diffusion is thus required to make it generally applicable.

To determine whether an expression for particle-phase diffusion is required in a regional model, an evaluation of the sensitivity of organic particle properties to diffusion is desirable. This study builds on previous investigations toward allowing such a sensitivity analysis, and enables it for the limiting case of particles with sufficiently low diffusivity that changes to the particle surface mole fraction of the partitioning component occur much more quickly than particle-phase diffusion. Work remains, however, to create a generally applicable realistic and efficient diffusion model for particulates containing organic components. Until this is achieved, studies of aerosol kinetic regimes conducted under limiting scenarios such as diffusion independent of composition, should be interpreted cautiously because of their limited applicability to the real atmosphere. In particular, the comparatively high abundance and high self-diffusion coefficient of water means that its role in plasticising or vitrifying particles through condensation and evaporation, respectively, must be accounted for when assessing the effect of particle-phase diffusion on partitioning.

Nomenclature

a	particle-phase bulk
A	area (m^2)
con	denotes a constant value
C	concentration (~~$\mathrm{mol\,m}^{-3}$~~$\mathrm{mol\,m}^{-3}$ (particle))
$\overline{C}$	concentration in bulk part of a phase (~~$\mathrm{mol\,m}^{-3}$~~$\mathrm{mol\,m}^{-3}$ (air))
$C*$	effective saturation vapour concentration ($\mathrm{mol\,m}^{-3}$ (air))
C_D	diffusion coefficient correction
D	diffusion coefficient ($\mathrm{m}^2\,\mathrm{s}^{-1}$)
eff	denotes an effective value
eq	equilibrium state
$\mathrm{Fi-PaD}$	Fick's Second Law solved by partial differential equation
g	gas-phase
i	a component
j	all components
k_n	chemical reaction rate ($\mathrm{m}^3\,\mathrm{molecule}^{-1}\,\mathrm{s}^{-1}$)
k_t	condensation sink rate (s^{-1})
K	mass transfer coefficient ($\mathrm{m\,s}^{-1}$)
m	index for size-bin
M	molar mass ($\mathrm{g\,mol}^{-1}$)
MOSAIC	Model for Simulating Aerosol Interactions and Chemistry
N	particle number concentration (m^{-3} air)
nv	non-volatile component
ρ	density ($\mathrm{g\,m}^{-3}$)
p_n	correction equation parameter
$_p$	subscript denotes particle-phase
r	radius (m)
rat	denotes a ratio
R_p	total particle radius (m)
s	particle-phase surface
sv	semi-volatile component
t	time (s)
t_e	e-folding time (s)
t_n	a time after n number of time steps (s)
v_d	deposition velocity ($\mathrm{m\,s}^{-1}$)
V_m	molar volume ($\mathrm{m}^3\,\mathrm{mol}^{-1}$)
x	mole fraction

Author contributions. S. O'Meara completed the practical work of the investigation and wrote the manuscript. R. A. Zaveri provided the MOSAIC code and assistance in its employment. All authors contributed to devising the methodology, result output and manuscript.

Competing interests. The authors declare that they have no conflict of interest.

Acknowledgements. The PhD of SO was funded by the Natural Environment Research Council award NE/K500859/1. This work was also funded by the Natural Environment Research Council award NE/M003531/1. Participation of RAZ in this study was supported by the US Department of Energy (DOE) Atmospheric System Research (ASR) Program under contract DE-AC06-76RLO 1830 at Pacific Northwest National Laboratory.

Appendix A

$\log_{10}({}^{D^0_{nv}}/{}_{D^0_{sv}})$	0	-2	-4	-6	-8	-10	-12
$\Delta x_{s,sv}$				p_1			
0.05	1.50	1.55	1.60	1.65	1.70	1.75	1.80
0.20	1.75	1.80	1.85	1.90	1.95	2.00	2.05
0.35	2.00	2.00	2.00	2.00	1.90	1.80	1.67
0.65	2.00	2.00	1.70	1.50	1.40	1.30	1.25
0.80	2.00	1.70	1.30	1.23	1.19	1.14	1.13
0.88	2.60	1.35	1.22	1.10	1.08	1.07	1.13
				p_2			
0.05	150.00	185.00	228.00	285.00	352.00	450.00	580.00
0.20	30.00	40.00	57.00	77.00	105.00	135.00	180.00
0.35	15.00	24.00	36.00	51.00	56.00	61.00	61.00
0.65	6.00	12.00	16.00	19.20	23.50	26.50	29.30
0.80	5.30	10.20	12.40	16.20	20.20	23.30	25.90
0.88	4.00	7.40	11.40	16.00	19.90	22.60	25.30
				p_3			
0.05	0.70	0.70	0.70	0.70	0.70	0.70	0.70
0.20	0.40	0.40	0.40	0.4 0	0.40	0.4 0	0.40
0.35	0.10	0.10	0.10	0.10	0.10	0.10	0.10
0.65	-0.30	-0.40	-0.40	-0.40	0.20	0.20	0.20
0.80	-2.30	-2.50	-1.50	-1.20	-0.80	-0.30	0.10
0.88	-2.50	-2.80	-1.50	-1.50	-1.50	-1.50	0.00

Table A1. Eq. 9 parameter values found for +ve $\Delta x_{s,sv}$.

$\log_{10}(^{D^0_{nv}}/_{D^0_{sv}})$	0	-4	-8	-12
$\Delta x_{s,sv}$		p_1		
-0.05	2.81	2.86	2.92	3.00
-0.20	3.23	3.53	3.46	2.00
-0.35	3.65	4.40	4.00	2.00
-0.65	5.00	8.00	5.00	2.00
-0.88	6.00	11.0	7.00	1.90
		p_2		
-0.05	8000.00	8000.00	8000.00	8000.00
-0.20	350.00	300.00	100.00	-1.60
-0.35	100.00	50.00	-1.00	-1.60
-0.65	23.00	12.00	-1.00	-0.40
-0.88	7.00	3.00	0.55	-0.20
		p_3		
-0.05	0.40	0.42	0.40	0.42
-0.20	0.32	0.41	0.50	0.52
-0.35	0.25	0.40	0.58	0.62
-0.65	0.00	0.50	0.67	0.76
-0.88	-0.10	0.58	0.78	0.85

Table A2. Eq. 9 parameter values found for -ve $\Delta x_{s,sv}$.

$\log_{10}(^{D^0_{nv}}/_{D^0_{sv}})$	0	-2	-4	-6	-8	-10	-12
p_i			Method Code				
p_1	00S	00S	00S	00S	00S	00S	00S
p_2	11L	11L	11L	11L	11L	11L	11L
p_3	00S	00S	00S	00L	00S	00S	00S
$\Delta x_{s,sv}$	$\geq 0.00 < 0.27$	$\geq 0.27 < 0.65$	≥ 0.65				
p_i			Method Code				
p_1	01L ($D^0_r \geq -3$) 01S ($D^0_r < -3$)	01L ($D^0_r \geq -3$) 01S ($D^0_r < -3$)	01L ($D^0_r \geq -3$) 01S ($D^0_r < -3$)				
p_2	01S ($D^0_r < -8$) 01L ($D^0_r \geq -8$)	11L ($D^0_r < -4$) 01L ($D^0_r \geq -4$)	11L				
p_3	01S	01S	01S				

Table A3. Interpolation method for parameters in eq. 9 (for +ve $\Delta x_{s,sv}$). Interpolation is done with respect to $\Delta x_{s,sv}$ first, followed by $\log_{10}(^{D^0_{nv}}/_{D^0_{sv}})$; the method for the former is given in the upper part of the table and the method for the latter is in the lower part. Note the method is dependent on the independent variable. Methods are represented by codes. The first number in each code is 1 if interpolation is done with respect to the $\log_{10}$ of parameter values, in which case the interpolation result must be raised to the power 10, and is 0 if no logarithm is taken. The second number in each code is 1 if the interpolation is done with respect to the $\log_{10}$ of the independent variable, and is 0 if no logarithm is taken. The final letter represents the form of the interpolation: L and S for linear and spline, respectively. For p_2, when interpolating with respect to $\log_{10}(^{D^0_{nv}}/_{D^0_{sv}})$, the interpolation method depends on the value of this variable, which is denoted D^0_r.

$\log_{10}(^{D^0_{nv}}/_{D^0_{sv}})$	0	-4	-8	-12
p_i		Method Code		
p_1	00L	00L	00L	00L
p_2	11L	11L	1(2)1L	1(2)0L
p_3	00L	00L	00L	00L
$\Delta x_{s,sv}$	$> -0.27 \leq 0.00$	$> -0.65 \leq -0.27$	≤ -0.65	
p_i		Method Code		
p_1	01L	01L	01L	
p_2	1(2.0)1S ($D^0_r < -8$)	1(2.0)1S ($D^0_r < -4$)	1(1.1)1S ($D^0_r \geq -6, \quad D^0_r \leq -4$)	
	01L ($D^0_r \geq -8$)	01L ($D^0_r \geq -4$)	1(2.0)1L ($D^0_r > -4, \quad D^0_r < -6$)	
p_3	1(2.0)1S	1(2.0)1S	1(2.0)1S	

Table A4. Interpolation method for parameters in eq. 9 (for -ve $\Delta x_{s,sv}$). Interpolation is done with respect to $\Delta x_{s,sv}$ first, followed by $\log_{10}(^{D^0_{nv}}/_{D^0_{sv}})$; the method for the former is given in the upper part of the table and the method for the latter is in the lower part. Note the method is dependent on the independent variable. Methods are represented by codes. The first number in each code is 1 if interpolation is done with respect to the $\log_{10}$ of parameter values, in which case the interpolation result must be raised to the power 10, and is 0 if no logarithm is taken. Because parameters are sometimes negative, to gain a real result from the logarithm, a constant must be added to the parameters first, if this is the case this constant is given in brackets beside the first code number (once interpolation is complete this constant is subtracted from the result after it has been raised to the power 10). The second number in each code is 1 if the interpolation is done with respect to the $\log_{10}$ of the independent variable, and is 0 if no logarithm is taken. The final element represents the form of the interpolation: L and S for linear and spline, respectively. For p_2, when interpolating with respect to $\log_{10}(^{D^0_{nv}}/_{D^0_{sv}})$, the interpolation method depends on the value of this variable, which is denoted D^0_r.

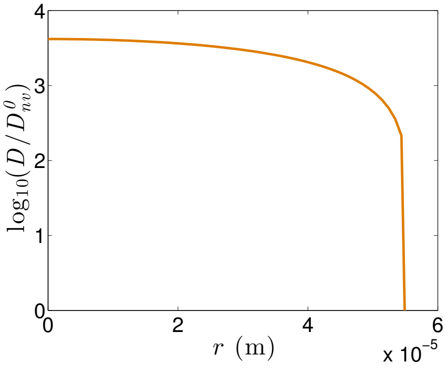

Figure A1. The logarithm of the ratio of the diffusion coefficient throughout an example particle to the self-diffusion coefficient of the non-volatile component, from the particle centre (at 0 m) to its surface. In this example, $\log_{10}(D^0_{nv}/D^0_{sv})$=-12, and $x_{s,sv,eq}$ = 0, and initial $x_{s,sv}$ = 0.88.

References

Barley, M., Topping, D., Lowe, D., Utembe, S., and McFiggans, G.: The sensitivity of secondary organic aerosol (SOA) component partitioning to the predictions of component properties-Part 3: Investigation of condensed compounds generated by a near-explicit model of VOC oxidation, Atmos. Chem. Phys., 11, 13 145–13 159, doi:10.5194/acp-11-13145-2011, 2011.

Berkemeier, T., Huisman, A., Ammann, M., Shiraiwa, M., Koop, T., and Pöschl, U.: Kinetic regimes and limiting cases of gas uptake and heterogeneous reactions in atmospheric aerosols and clouds: a general classification scheme, Atmos. Chem. Phys., 13, 6663–6686, doi:10.5194/acp-13-6663-2013, 2013.

Boucher, O., Randall, D., Artaxo, P., Bretherton, C., Feingold, G., Forster, P., Kerminen, V.-M., Kondo, Y., Liao, H., Lohmann, U., Rasch, P., Satheesh, S., Sherwood, S., Stevens, B., and Zhang, X.: Clouds and Aerosols, in: Climate Change 2013: The Physical Science Basis. Contribution of Working Group I to the Fifth Assessment Report of the Intergovernmental Panel on Climate Change, edited by Stocker, T., Qin, D., Plattner, G.-K., Tignor, M., Allen, S., Boschung, J., Nauels, A., Xia, Y., Bex, V., and Midgley, P., Cambridge University Press, Cambridge, United Kingdom and New York, NY, USA, 2013.

Crank, J.: The Mathematics of Diffusion, Clarendon Press, Oxford, 2 edn., 1975.

Donahue, N., Robinson, A., Stanier, C., and Pandis, S.: Coupled partitioning, dilution and chemical ageing of semivolatile organics, Environ. Sci. Technol., 40, 2635–2643, doi:10.1021/es052297c, 2006.

Ehn, M., Thornton, J., Kleist, E., Sipilä, M., Junninen, H., Pullinen, I., Springer, M., Rubach, F., Tillmann, R., Lee, B., Lopez-Hilfiker, F., Andres, S., Acir, I., Rissanen, M., Jokinen, T., Schobesberger, S., Kangasluoma, J., Kontkanen, J., Nieminen, T., Kurtén, T., Nielsen, L. B., Jørgensen, S., Kjaergaard, H., Canagaratna, M., Maso, M., Berndt, T., Petäjä, T., Wahner, A., Kerminen, V., Kulmala, M., Worsnop, D., Wildt, J., and Mentel, T.: A large source of low-volatility secondary organic aerosol, Nature, 506, 476–479, doi:10.1038/nature13032, 2014.

Fiore, A., Naik, V., Spracklen, D., Steiner, A., Unger, N., Prather, M., Bergmann, D., Cameron-Smith, P., Cionni, I., Collins, W., Dalsøren, S., Eyring, V., Folberth, G., Ginoux, P., Horowitz, L., Josse, B., Lamarque, J., MacKenzie, I., Nagashima, T., O'Connor, F., Righi, M., Rumbold, S., Shindell, D., Skeie, R., Sudo, K., Szopa, S., Takemura, T., and Zeng, G.: Global air quality and climate, Chem. Soc. Rev., 41, 6663–6683, 2012.

Glotfelty, T., Zhang, Y., Karamchandani, P., and Streets, D.: Changes in future air quality, deposition, and aerosol-cloud interactions under future climate and emission scenarios, Atmos. Environ., doi:10.1016/j.atmosenv.2016.05.008, 2016.

Jacobson, M. and Streets, D.: Influence of future anthropogenic emissions on climate, natural emissions, and air quality, J. Geophys. Res., 114, D08 118, doi:10.1029/2008JD011476, 2009.

Koop, T., Bookhold, J., Shiraiwa, M., and Pöschl, U.: Glass transition and phase state of organic compounds: dependency on molecular properties and implications for secondary organic aerosols in the atmosphere, Phys. Chem. Chem. Phys., 13, 19 238–19 255, doi:10.1039/c1cp22617g, 2011.

Krishna, R. and Wesselingh, J.: The Maxwell-Stefan approach to mass transfer, Chem. Eng. Sci., 52, 861–911, doi:10.1016/S0009-2509(96)00458-7, 1997.

Kroll, J. and Seinfeld, J.: Chemistry of secondary organic aerosol: formation and evolution of low-volatility organics in the atmosphere, Atmos. Environ., 42, 3593–3624, doi:10.1016/j.atmosenv.2008.01.003, 2008.

Lienhard, D., Huisman, A., Bones, D., Te, Y., Luo, B., Krieger, U., and Reid, J.: Retrieving the translational diffusion coefficient of water from experiments of single levitated aerosol droplets, Phys. Chem. Chem. Phys., 16, 16 677–16 683, doi:10.1039/c4cp01939c, 2014.

Mai, H., Shiraiwa, M., Flagan, R., and Seinfeld, J.: Under what conditions can equilibrium gas-particle partitioning be expected to hold in the atmosphere?, Environ. Sci. Technol., 49, 11 485–11 491, doi:10.1021/acs.est.5b02587, 2015.

O'Meara, S., Topping, D., and McFiggans, G.: The rate of equilibration of viscous aerosol particles, Atmos. Chem. Phys., 16, 5299–5313, doi:10.5194/acp-16-5299-2016, 2016.

Price, C., Mattsson, J., Zhang, Y., Bertram, A., Davies, J., Grayson, J., , Martin, S., O'Sullivan, D., Reid, J., Rickards, A., and Murray, B.: Water diffusion in atmospherically relevant α-pinene secondary organic material, Chem. Sci., 6, 4876–4883, doi:10.1039/C5SC00685F, 2015.

Saukko, E., Lambe, A., Massoli, P., Koop, T., Wright, J., Croasdale, D., Pedernera, D., Onasch, T., Laaksonen, A., Davidovits, P., Worsnop, D., and Virtanen, A.: Humidity-dependent phase state of SOA particles from biogenic and anthropogenic precursors, Atmos. Chem. Phys., 12, 7517–7529, doi:10.5194/acp-12-7517-2012, 2012.

Sehmel, G.: Particle and gas dry deposition: a review, Atmos. Environ., 14, 983–1011, doi:10.1016/0004-6981(80)90031-1, 1980.

Seinfeld, J. and Pandis, S.: Atmospheric chemistry and physics: from air pollution to climate change, Wiley, Hoboken, N.J., 2 edn., 2006.

Sellegri, K., Hanke, M., Umann, B., Arnold, F., and Kulmala, M.: Measurements of organic gases during aerosol formation events in the boreal forest atmosphere during QUEST, Atmos. Chem. Phys., 5, 373–384, doi:10.5194/acp-5-373-2005, 2005.

Shiraiwa, M., Pfrang, C., Koop, T., and Pöschl, U.: Kinetic multi-layer model of gas-particle interactions in aerosols and clouds (KM-GAP): linking condensation, evaporation and chemical reactions of organics, oxidants and water, Atmos. Chem. Phys., 12, 2777–2794, doi:10.5194/acp-12-2777-2012, 2012.

Smith, G., Woods, E., Baer, T., and Miller, R.: Aerosol uptake described by numerical solution of the diffusion-reaction equations in the particle, J. Phys. Chem. A, 107, 9582–9587, doi:10.1021/jp021843a, 2003.

Starr, F., Sciortino, F., and Stanley, H.: Dynamics of simulated water under pressure, Phys. Rev. E, 60, 6757–6768, doi:10.1103/PhysRevE.60.6757, 1999.

Steimer, S., Krieger, U., Te, Y.-F., Lienhard, D., Huisman, A., B.P.Luo, Ammann, M., and Peter, T.: Electrodynamic balance measurements of thermodynamic, kinetic, and optical aerosol properties inaccessible to bulk methods, Atmos. Meas. Tech., 8, 2397–2408, doi:10.5194/amt-8-2397-2015, 2015.

Taylor, R. and Krishna, R.: Multicomponent Mass Transfer, John Wiley and Sons, Inc., New York, 1993.

Topping, D., Barley, M., and McFiggans, G.: The sensitivity of Secondary Organic Aerosol (SOA) component partitioning to the predictions of component properties-Part 2: Determination of the particle hygroscopicity and its dependence on "apparent" volatility, Atmos. Chem. Phys., 11, 7767–7779, doi:10.5194/acp-11-7767-2011, 2011.

Topping, D., Barley, M., and McFiggans, G.: Including phase separation in a unified model to calculate partitioning of vapours to mixed inorganic-organic aerosol particles, Faraday Discuss., 165, 273–288, doi:10.1039/C3FD00047H, 2013.

Tröstl, J., Chuang, W., Gordon, H., Heinritzi, M., Yan, C., Molteni, U., Ahlm, L., Frege, C., Bianchi, F., Wagner, R., Simon, M., Lehtipalo, K., Williamson, C., Craven, J., Duplissy, J., Adamov, A., Almeida, J., Bernhammer, A.-K., Breitenlechner, M., Brilke, S., Dias, A., Ehrhart, S., Flagan, R., Franchin, A., Fuchs, C., Guida, R., Gysel, M., Hansel, A., Hoyle, C., Jokinen, T., Junninen, H., Kangasluoma, J., Keskinen, H., Kim, J., Krapf, M., Kürten, A., Laaksonen, A., Lawler, M., Leiminger, M., Mathot, S., Möhler, O., Nieminen, T., Onnela, A., Petäjä, T., Piel, F., Miettinen, P., Rissanen, M., Rondo, L., Sarnela, N., Schobesberger, S., Sengupta, K., Sipilä, M., Smith, J., Steiner, G., Tomé, A., Virtanen, A., Wagner, A., Weingartner, E., Wimmer, D., Winkler, P., Ye, P., Carslaw, K., Curtius, J., Dommen, J., Kirkby, J., Kulmala, M., Riipinen, I., Worsnop, D., Donahue, N., and Baltensperger, U.: The role of low-volatility organic compounds for initial particle growth in the atmosphere, Nature, 506, 527–531, doi:10.1038/nature18271, 2016.

Vaden, T., Imre, D., Beránek, J., Shrivastava, M., and Zelenyuk, A.: Evaporation kinetics and phase of laboratory and ambient secondary organic aerosol, P. Natl. Acad. Sci. USA, 108, 2190–2195, doi:10.1073/pnas.1013391108, 2011.

Vignes, A.: Diffusion in binary solutions, Ind. Eng. Chem. Fund., 5, 189–199, doi:10.1021/i160018a007, 1966.

Virtanen, A., J.Joutsensaari, Koop, T., Kannosto, J., Yli-Pirilä, P., Leskinen, J., Mäkelä, J., Holopainen, J., Pöschl, U., Kulmala, M., Worsnop, D., and Laaksonen, A.: An amorphous solid state of biogenic secondary organic aerosol particles, Nature, 467, 824–827, doi:10.1038/nature09455, 2010.

Whitehead, J., Dorsey, J., Gallagher, M., Flynn, M., McFiggans, G., and Carpenter, L.: Particle fluxes and condensational uptake over sea ice during COBRA, J. Geophys. Res., 117, D15 202, doi:10.1029/2012JD017798, 2012.

Zaveri, R., Easter, R., Fast, J., and Peters, L.: Model for Simulating Aerosol Interactions and Chemistry (MOSAIC), J. Geophys. Res., 113, D13 204, doi:10.1029/2007JD008782, 2008.

Zaveri, R., Easter, R., Shilling, J., and Seinfeld, J.: Modeling kinetic partitioning of secondary organic aerosol and size distribution dynamics: representing effects of volatility, phase state, and particle-phase reaction, Atmos. Chem. Phys, 14, 5153–5181, doi:doi:10.5194/acp-14-5153-2014, 2014.

Ziemann, P. and Atkinson, R.: Kinetics, products, and mechanisms of secondary organic aerosol formation, Chem. Soc. Rev., 41, 6582–6605, doi:10.1039/c2cs35122f, 2012.

Zobrist, B., Marcolli, C., Pedernera, D., and Koop, T.: Do atmospheric aerosols form glasses?, Atmos. Chem. Phys., 8, 5221–5244, doi:10.5194/acp-8-5221-2008, 2008.

Zobrist, B., Soonsin, V., Luo, B., Krieger, U., Marcolli, C., Peter, T., and Koop, T.: Ultra-slow water diffusion in aqueous sucrose glasses, Phys. Chem. Chem. Phys., 13, 3514–3526, doi:10.1039/c0cp01273d, 2011.

Zuend, A., Marcolli, C., Luo, B., and Peter, T.: A thermodynamic model of mixed organic-inorganic aerosols to predict activity coefficients, Atmos. Chem. Phys., 8, 4559–4593, doi:10.5194/acp-8-4559-2008, 2008.